Histaprodifens: Synthesis, Pharmacological in Vitro Evaluation, and Molecular Modeling of a New Class of Highly Active and Selective Histamine H_1-Receptor Agonists†

Sigurd Elz,§ Kai Kramer,§ Heinz H. Pertz,§ Heiner Detert,# Anton M. ter Laak,⊥ Ronald Kühne,⊥ and Walter Schunack*,§

Institut für Pharmazie, Freie Universität Berlin, Königin-Luise-Strasse 2+4, D-14195 Berlin (Dahlem), Germany, Institut für Organische Chemie, Johannes Gutenberg-Universität, J.-J. Becherweg 18-20, D-55099 Mainz, Germany, and Forschungsinstitut für Molekulare Pharmakologie, Alfred-Kowalke-Strasse 4, D-10315 Berlin, Germany

Received April 12, 1999

A new class of histamine analogues characterized by a 3,3-diphenylpropyl substituent at the 2-position of the imidazole nucleus has been prepared outgoing from 4,4-diphenylbutyronitrile (**4b**) via cyclization of the corresponding methyl imidate **5b** with 2-oxo-4-phthalimido-1-butyl acetate or 2-oxo-1,4-butandiol in liquid ammonia, followed by standard reactions. The title compounds displayed partial agonism on contractile H_1 receptors of the guinea-pig ileum and endothelium-denuded aorta, respectively, except **10** (*histaprodifen*; 2-[2-(3,3-diphenylpropyl)-1*H*-imidazol-4-yl]ethanamine) which was a full agonist in the ileum assay. While **10** was equipotent with histamine (**1**), methylhistaprodifen (**13**) and dimethylhistaprodifen (**14**) exceeded the functional potency of **1** by a factor of 3−5 (**13**) and 2−3 (**14**). Compounds **10** and **13**−**17** relaxed precontracted rat aortic rings (intact endothelium) with relative potencies of 3.3- up to 28-fold (compared with **1**), displaying partial agonism as well. Agonist effects were sensitive to blockade by the selective H_1-receptor antagonist mepyramine ($pA_2 \approx 9$ (guinea-pig) and $pA_2 \approx 8$ (rat aorta)). The affinity of **10** and **13**−**17** for guinea-pig H_1 receptors increased 20- to 100-fold compared with **1**. Two lower homologues of **10** were weak partial H_1-receptor agonists while two higher homologues of **10** were silent antagonists endowed with micromolar affinity for rat and guinea-pig H_1 receptors. In functional selectivity experiments, **10**, **13**, and **14** did not stimulate H_2, H_3, and several other neurotransmitter receptors. They displayed only low to moderate affinity for these sites ($pA_2 < 6$). For a better understanding of structure−activity relationships, the interaction of **1** and **10**, **13** and **14** within the transmembrane (TM) domains of the human histamine H_1 receptor were studied using molecular dynamics simulations. Remarkable differences were found between the binding modes of **10**, **13**, and **14** and that of **1**. The imidazole ring of **10**, **13**, and **14** was placed 'upside down' compared with **1**, making the interaction of the N^{π}-atom with Tyr431 possible. This new orientation was mainly caused by the space filling substitution at the 2-position of the imidazole ring and influenced the location of the protonated N^{α}-atom which was positioned more between TM III and TM VI. This orientation can explain both the increased relative potency and the maximum effect of **10**, **13**, and **14** compared with **1**. Compound **13** (*methylhistaprodifen*; N^{α}-methyl-2-[2-(3,3-diphenylpropyl)-1*H*-imidazol-4-yl]ethanamine) is the most potent histamine H_1-receptor agonist reported so far in the literature and may become a valuable tool for the study of physiological and pathophysiological H_1-receptor-mediated effects.

Introduction

During the last 15 years it has been demonstrated that histamine (**1**, Chart 1) exerts an immense diversity of physiological and pathophysiological effects via interaction with histamine H_1 receptors. For example, **1** seems to be an anticonvulsive inhibitory transmitter[4,5] and a central inhibitor of intestinal transit.[6] Furthermore, **1** plays an important role in the pathogenesis of coronary spasms[7−9] and in the control of sleep and

Chart 1

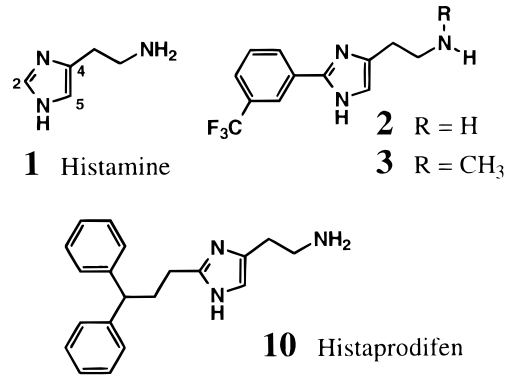

† Presented in part at the XXVIth Meeting of the European Histamine Research Society, Sevilla, Spain, May 14−17, 1997;[1] XXVIIth Meeting of the European Histamine Research Society, Lódz, Poland, May 20−23, 1998;[2] and XIIIth International Congress of Pharmacology, Munich, Germany, July 26−31, 1998.[3]

* To whom correspondence should be addressed. Phone: +49-30-838 53278. Fax: +49-30-838 52242. E-mail: sieker@schunet1.pharmazie.fu-berlin.de.

§ Institut für Pharmazie.

Institut für Organische Chemie.

⊥ Forschungsinstitut für Molekulare Pharmakologie.

10.1021/jm991056a CCC: $19.00
Published on Web 03/04/2000

Chart 2. H_1-Receptor Antagonists Therapeutically Used as Antiallergics, Characterized by a Diphenylmethyl Substituent

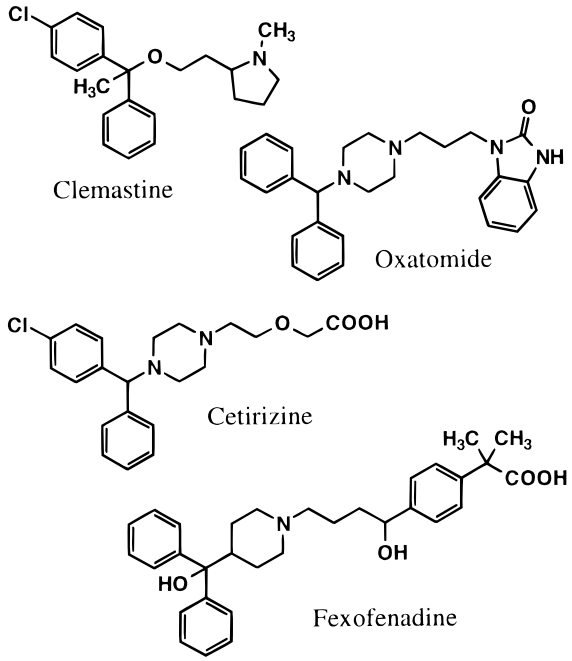

waking state.[10] Unfortunately, the studies of the effects of **1** have been limited by the lack of highly potent and selective histamine H_1-receptor agonists. While for the histamine H_2 and H_3 receptors highly potent agonists have been described which exceed the potency of the endogeneous ligand by a factor of 10 to 100,[11−14] the search for potent high-affinity H_1-receptor agonists has been an arduous task for several decades.[15,16]

One of the first synthetic H_1-receptor agonists was 2-(2-thiazolyl)ethanamine. This compound is commonly used as an H_1-receptor agonist although it displays only moderate potency and selectivity for this receptor subtype. It has previously been shown that the attachment of a small alkyl residue (2-methylhistamine[17,18]) or a phenyl residue (2-phenylhistamine[19]) to the 2-position of histamine[20] affords agonists with moderate activity but higher selectivity for H_1 receptors. A remarkable increase in H_1-receptor agonist activity has been achieved by the introduction of different substituents in the meta position of the phenyl ring. Finally, this has led to 2-(3-trifluoromethylphenyl)histamine (**2**), a compound that slightly exceeds the potency of histamine on the guinea-pig ileum (relative potency: 128%; histamine 100%).[21] On the basis of the findings that, in a series of N^{α}-substituted 2-methylhistamines, N^{α}-mono- and dimethylation caused improved H_1-receptor agonist potency,[22] we have reported the synthesis of N^{α}-methyl-2-(3-trifluoromethylphenyl)histamine (**3**).[23] This compound acts as a full H_1-receptor agonist in the guinea-pig ileum assay with a relative potency of 174%.

Some 2-substituted histamine derivatives have recently been found to stimulate G-proteins in a receptor-independent manner.[24,25] A common feature of some clinically used H_1-receptor antagonists belonging to the first, second, and third generation[26] is the presence of a diphenylmethyl substituent which is believed to confer high receptor affinity on these H_1 antihistamines (Chart 2). When a series of potentially G-protein-stimulatory histamine analogues combining a histamine moiety with a ω,ω-diphenylalkyl substituent were screened for H_1-receptor affinity, compound **10** (Chart 1, 2-[2-(3,3-diphenylpropyl)imidazol-4-yl]ethanamine, *histaprodifen*) was surprisingly identified as an H_1-receptor agonist, being equipotent with **1**.[1,2]

Scheme 1. Synthesis of Nitriles **4a**−**d**[a]

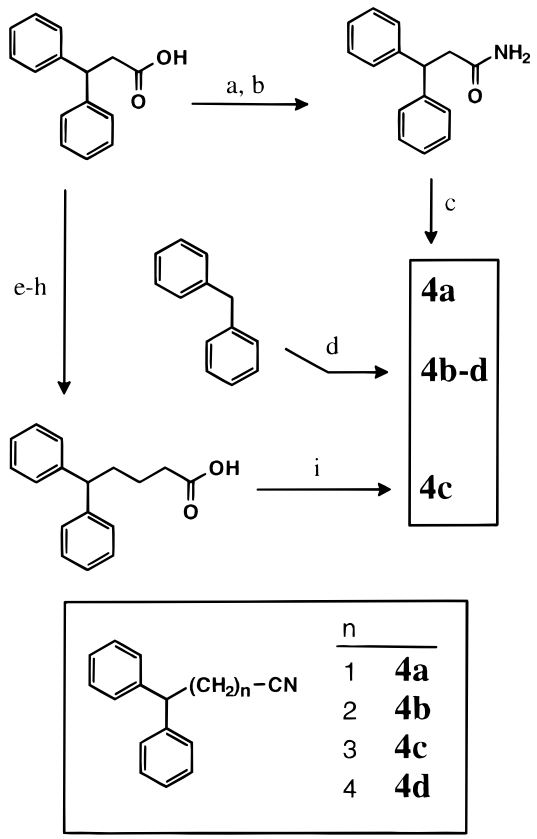

[a] (a) $SOCl_2$; (b) liq. NH_3; (c) P_4O_{10}; (d) KNH_2, liq. NH_3, Et_2O (−70 °C), $Br(CH_2)_2CN$ or $Br(CH_2)_3CN$ or $Cl(CH_2)_4CN$; (e) $LiAlH_4$, Et_2O, column chromatography; (f) $SOCl_2$, 4-DMAP (cat.), CH_2Cl_2, column chromatography; (g) diethyl malonate, NaH, NaI (cat.), DMF, KOH; (h) 180 °C (in vacuo); (i) CSI ($ClSO_2N{=}C{=}O$),[30] CH_2Cl_2.

The present report deals with the synthesis of histaprodifen (**10**), homologous compounds, and N^{α}-substituted analogues, their in vitro characterization in several functional H_1-receptor assays, and their selectivity, respectively. Furthermore, the putative interaction of **1** and the most potent histaprodifens with the helical transmembrane (TM) domains of the human histamine H_1 receptor (hH1R) has been studied using molecular dynamics (MD) simulations. The TM domain model of the hH1R was derived from electron-density mapping of frog rhodopsin.[27]

Chemistry

2-(ω,ω-Diphenylalkyl)imidazoles were prepared from the respective ω,ω-diphenylalkannitriles **4a**−**d** (Scheme 1) by cyclization of the corresponding methyl imidates **5a**−**d** with appropriate C_4 synthons in liquid ammonia[28] in order to avoid a multistep procedure for the construction of the histamine side chain (Scheme 2).

4,4-Diphenylbutyronitrile (**4b**) and higher homologues **4c** and **4d** were obtained from a potassium amide/liquid ammonia solution of diphenylmethane by alkylation

Scheme 2. Synthesis and Structure of Final Compounds **9**−**17**[a,b] Including Structure of the Previously Described **8**[19]

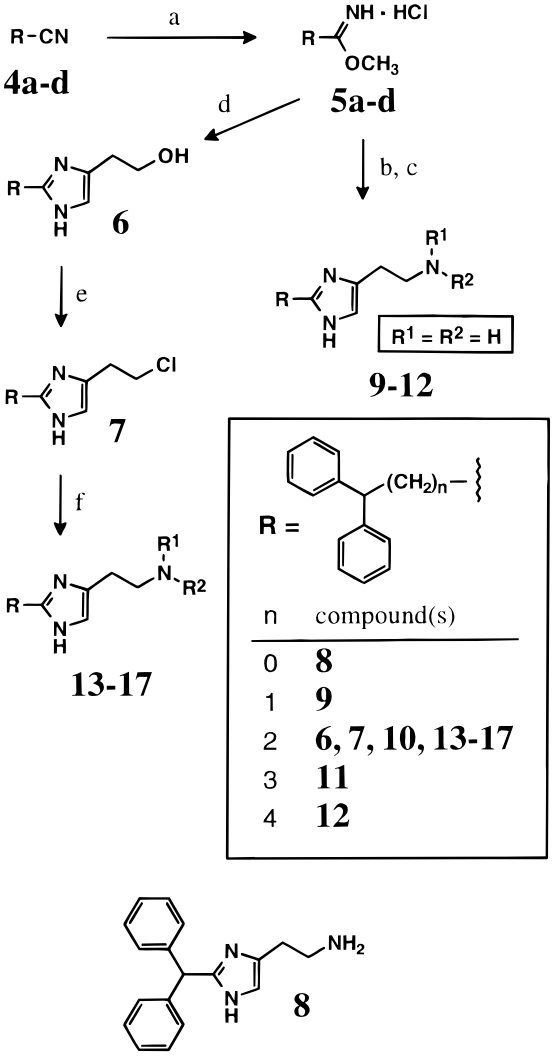

[a] (a) MeOH, $SOCl_2$ (−30 °C); (b) 2-oxo-4-phthalimido-1-butyl acetate,[32] liq. NH_3; (c) N_2H_4; (d) 2-oxobutan-1,4-diol,[31] liq. NH_3; (e) $SOCl_2$; (f) NHR^1R^2, KI, K_2CO_3, H_2O/EtOH, chromatographic purification. [b]For R^1 and R^2, see also Table 1.

with appropriate *ω*-bromo- or *ω*-chloroalkannitriles (Scheme 1). 3,3-Diphenylpropionitrile (**4a**) was synthesized from commercially available 3,3-diphenylpropionic acid.[29] This acid also served as starting material for an alternative preparation of **4c** via C-alkylation of diethyl malonate with 1-chloro-3,3-diphenylpropane, saponification of the diester, and subsequent monodecarboxylation. The resulting 5,5-diphenylvaleric acid was converted into the nitrile **4c** by treatment with chlorosulfonylisocyanate.[30]

Reaction of the nitriles **4a**−**c** with an excess of dry methanol and thionyl chloride afforded methyl imidates **5a**−**d**. The substituted methyl butyrimidate **5b** was cyclized to imidazole ethanol **6** by treatment with 2-oxobutan-1,4-diol in liquid ammonia. 2-Oxobutan-1,4-diol was readily available by mercury(II)-catalyzed addition of water to butin-1,4-diol.[31] Imidazole ethanol **6** was converted to the corresponding chloroethane **7** which yielded N^{α}-substituted 2-(3,3-diphenylpropyl)-histamine derivatives **13**−**17** upon treatment with excess amine. Cyclization of **5a**−**d** in the presence of 2-oxo-4-phthalimido-1-butyl acetate[32] in liquid ammonia gave the primary amines **9**−**12** after deprotection. After workup, the target compounds were purified by chromatographic methods and crystallized as dihydrogen oxalates or dihydrogen maleates, respectively.

Biological Results and Discussion

H_1-Receptor Agonism on the Isolated Guinea-Pig Ileum. The novel histamine derivatives **9**−**17** were routinely examined for H_1-histaminergic properties on the guinea-pig ileum preparation (Table 1). In the series of homologues **8**−**12**, only histaprodifen (**10**) displayed contractile potency comparable with that of **1**, while the lower homologues **8**[19] and **9** were partial agonists with reduced potency (8% and 0.5%) and diminished affinity (pK_P = 5.4 and 3.9; for pK_P see below). Both higher homologues of **10**, viz. **11** and **12**, were devoid of agonist effects but, like **10**, possess micromolar affinity for the H_1 receptor ($pA_2 \approx 6$).

While the agonist potency of **10** and **15**−**17** was similar to that of **1**, the methyl derivatives of **10**, viz. methylhistaprodifen (**13**) and dimethylhistaprodifen (**14**), were significantly more potent than **1** by an approximate factor of 3.5 and 2.5, respectively. Hence compound **13** is the most potent H_1-receptor agonist on the guinea-pig ileum reported in the literature. With regard to the obtained maximal contraction, substituents bulkier than methyl, e.g., ethyl (**15**) and cyclopropyl (**16**), or a tertiary amine structure (**14**, **17**) lead to partial agonism, while **13** virtually displays a full agonist behavior on the ileal preparation. Affinity constants around 1 nM ($pA_2 \approx 9$) were calculated for the reference H_1-receptor antagonist mepyramine when the interaction of this compound with the new agonists **10** and **13**−**17** was studied (Table 5). Increasing concentrations of mepyramine resulted in a depression of the concentration−effect curves of the respective agonist (Figure 1, upper panel) which is often seen for H_1-receptor agonists with low or missing receptor reserve. This phenomenon may be the result of a 'hemi-equilibrium' state between agonist and antagonist[21,33] and indicates slow kinetics of the drugs involved. Indeed the ileal contractions elicited by **10** and **13**−**17**, which are rather lipophilic molecules, developed less rapidly compared with histamine, especially when mepyramine was present. Nonetheless the concentration-dependent rightward shift of the curves for **10** induced by mepyramine led to a Schild plot slope[34] of unity (Figure 1, upper panel). When the contractile response evoked by **10** and **13**−**17** was allowed to fade to a more or less constant level, a rightward displacement of a following concentration−effect curve for histamine could be observed (Figure 1, lower panel). Analysis of this rightward displacement gave an estimate of the dissociation constant (pK_P) of the partial-agonist/receptor complex[35,36] which lies in the micromolar range (Table 1). Compared with histamine (pK_i = 4.4 on guinea-pig cerebellar membranes[21]), the affinity of the members of the described histaprodifen series was approximately increased by a factor of 20−100.

H_1-Receptor Agonism on the Isolated Guinea-Pig Aorta. The most potent histaprodifens **10**, **13**, **14**, and **16** were studied in an arterial, endothelium-denuded guinea-pig preparation for their ability to evoke

Table 1. Contraction of Guinea-Pig Ileal Whole Segments by Histamine and Histaprodifens **8**−**17**[a]

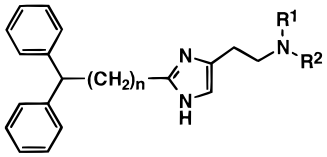

				agonism					antagonism vs histamine		
compd	*n*	R^1	R^2	N^b	$pEC_{50} \pm SEM$	relative potency	(95% confidence limits)	$E_{max} \pm SEM$	N^b	$pK_P{}^c \pm SEM$	c^d [μM]
8	0	H	H	7	5.59 ± 0.11	8	(4−15)	28 ± 4	5	5.37 ± 0.03	100
9	1	H	H	13	4.39 ± 0.05	0.5	(0.4−0.6)	50 ± 6	5	3.87 ± 0.08	100
10	2	H	H	34	6.74 ± 0.02	111	(99−124)	100[e]	12	6.04 ± 0.05	3−30[f]
11	3	H	H	13				2 ± 1	10	5.94 ± 0.04[g]	3−10
12	4	H	H	5				0	5	6.21 ± 0.02[h]	5
13	2	CH_3	H	19	7.24 ± 0.02	343	(308−382)	99 ± 1[i]	13	6.45 ± 0.04	30
14	2	CH_3	CH_3	16	7.08 ± 0.04	242	(199−295)	89 ± 1	16	6.40 ± 0.03	30
15	2	C_2H_5	H	10	6.52 ± 0.04	65	(53−81)	89 ± 2	6	5.75 ± 0.09	20
16	2	cC_3H_5	H	9	6.83 ± 0.04	134[j]	(111−162)	64 ± 2	10	6.17 ± 0.05	1−3
17	2	$-(CH_2)_4-$		8	6.53 ± 0.05	67	(51−88)	28 ± 5	8	6.52 ± 0.05	30
histamine				>100	6.70 ± 0.02	100		100			

[a] All experiments carried out in the presence of 0.1 μM atropine. [b] Number of experiments. [c] Negative logarithm of the partial-agonist/receptor dissociation constant K_P.[35,36] [d] Concentration of partial agonist or antagonist. Incubation time 5−10 min (**10**−**14**, **16**), 3 min (**15**), and 1 min (**8**, **9**, **17**), respectively. [e] Mean not significantly different from 100 (99.4 ± 0.4, $P > 0.05$). [f] Analyzed by Kaumann-Marano plot,[36] see Figure 1 (lower panel). [g] pA_2 value. When calculated as pK_P: 5.98 ± 0.04. [h] pA_2 value. [i] Mean significantly different from 100 (98.7 ± 0.5, $P < 0.02$). [j] Significantly different from 100 ($P < 0.01$).

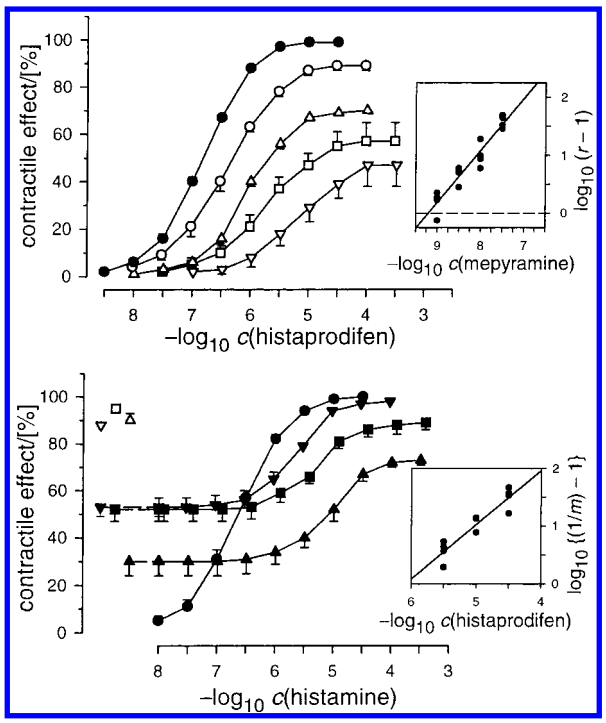

Figure 1. *Upper panel:* Contraction of guinea-pig ileum (whole segments) by histaprodifen (**10**) in the absence (●, $n = 17$, $E_{max} = 100\%$) and presence of the competitive H_1-receptor antagonist mepyramine [nM]: 1 (○, $n = 5$, $E_{max} = 89 \pm 2\%$), 3 (△, $n = 4$, 70 ± 1%), 10 (□, $n = 4$, 57 ± 8%), and 30 (▽, $n = 4$, 47 ± 9%). *Inset:* The Schild plot for mepyramine yielded a straight line of slope unity (0.90 ± 0.06, $n = 17$, not significantly different from 1.00) and a full pA_2 value of 9.11 ± 0.04. *Lower panel:* Contraction of guinea-pig ileum (whole segments) by histamine in the absence (●, $n = 10$) and presence of histaprodifen (**10**) [μM] (incubation time, $E_{max} \pm$ SEM induced by histamine): 3 (▼, 10 min, 98 ± 1%), 10 (■, 10 min, 89 ± 3%), and 30 (▲, 3 min, 73 ± 2%), respectively ($n = 4$ each). The initial response to **10** (open symbols) faded during the incubation period (closed symbols below). *Inset:* The Kaumann-Marano plot[36] for **10** gave a straight line of slope unity (0.94 ± 0.12, $n = 12$, not significantly different from 1.00) and a pK_P value of 6.04 ± 0.05.

H_1-receptor-mediated vasoconstriction. In the absence of $PGF_{2\alpha}$,[21,37] aortic rings displayed low sensitivity for **1**, and **10**, **13**, **14**, and **16** had lower pEC_{50} values compared with the ileum assay, too (Table 2). All compounds were partial agonists (relative maximum effects < 75%, Figure 2, upper panel). pEC_{50} values echoed pK_P values obtained on the ileum preparation of the same species. The relative maximum effect of **10**, **13**, and **14** increased to 80−90% when the aortic preparations were precontracted by a threshold concentration of $PGF_{2\alpha}$ (Figure 2, lower panel). The sensitization was typically characterized by an increase of pEC_{50} values for histaprodifens and **1** ($\Delta pEC_{50} \approx 0.8$, Table 3). Perfectly matching the ileum data, **10** was virtually equipotent with **1** under both experimental conditions, and **13** and **14** exceeded the potency of **1** by an approximate factor of 4.3 and 2.7, respectively. In both experimental sets the contractile effects were susceptible to specific blockade by mepyramine, yielding pA_2 values around 9 (Table 5). Under both experimental conditions the higher homologues **11** and **12** displayed H_1-receptor antagonism comparable with the ileum data ($pA_2 \approx 6.0$).

H_1-Receptor Agonism on the Isolated Rat Aorta with Intact Endothelium. Histamine relaxes rat aortic segments precontracted with noradrenaline[38,39] or phenylephrine[40] via the release of nitric oxide, provided that an intact endothelium is present. Since some histaprodifens displayed moderate α_{1D}-adrenoceptor blocking potency (see below), U46619, a TP(thromboxane-A_2)-receptor agonist, was used as vasoconstrictor agent. Histamine as well as the histaprodifens **10** and **13**−**17** exerted a vasodilator response on rat aortic rings submaximally and stably precontracted with U46619 (Table 4). Compared to the guinea-pig tissues, the endothelial H_1 receptor displayed substantially lower sensitivity for **1** ($pEC_{50} = 5.35$) while the pEC_{50} values of the new agonists remained in the range of 6−7, leading to increased relative potencies of 331−2825%. The rank order of potency was similar to that obtained

Table 2. Contraction of Endothelium-Denuded Guinea-Pig Aortic Segments (Primed with Histamine) by **1** and Histaprodifens **10**−**14** and **16**[a]

compd	N[b]	$pEC_{50} \pm$ SEM	relative potency	(95% confidence limits)	E_{max}[c] ± SEM
10	12	5.71 ± 0.02	115[d]	(105−126)	72 ± 2
11	6		[$pA_2 = 5.80 \pm 0.05$	(5.68−5.93)]	0[e]
12	6		[$pA_2 = 6.00 \pm 0.10$	(5.75−6.25)]	0[e]
13	12	6.31 ± 0.03	458[d]	(399−526)	63 ± 2
14	12	6.08 ± 0.04	272[d]	(226−326)	54 ± 2
16	9	5.64 ± 0.03	97	(85−111)	52 ± 3
1	74	5.65 ± 0.02	100		100

[a] For structure, see Table 1. [b] Number of experiments. [c] Formerly termed 'intrinsic activity'.[48] Second curves of histamine controls arbitrarily set to 100%. [d] Significantly more potent than histamine ($P < 0.01$). [e] At 10 μM.

Table 3. Contraction of Endothelium-Denuded Guinea-Pig Aortic Segments (Precontracted with a Threshold Concentration of $PGF_{2\alpha}$) by **1** and Histaprodifens **10**−**14**[a]

compd	N[b]	$pEC_{50} \pm$ SEM	relative potency	(95% confidence limits)	E_{max}[c] ± SEM
10	11	6.51 ± 0.04	101	(81−126)	84 ± 2
11	5		[$pA_2 = 5.92 \pm 0.10$	(5.66−6.19)]	0[d]
12	5		[$pA_2 = 6.08 \pm 0.12$	(5.76−6.40)]	0[d]
13	13	7.11 ± 0.07	410[e]	(296−569)	89 ± 4
14	11	6.92 ± 0.07	265[e]	(183−385)	85 ± 4
1	25	6.50 ± 0.04	100		100

[a] For structure, see Table 1. [b] Number of experiments. [c] Formerly termed 'intrinsic activity'.[48] Maximum of histamine controls (relative to contraction evoked by 10 μM $PGF_{2\alpha}$) arbitrarily set to 100%. [d] At 10 μM. [e] Significantly more potent than histamine ($P < 0.01$).

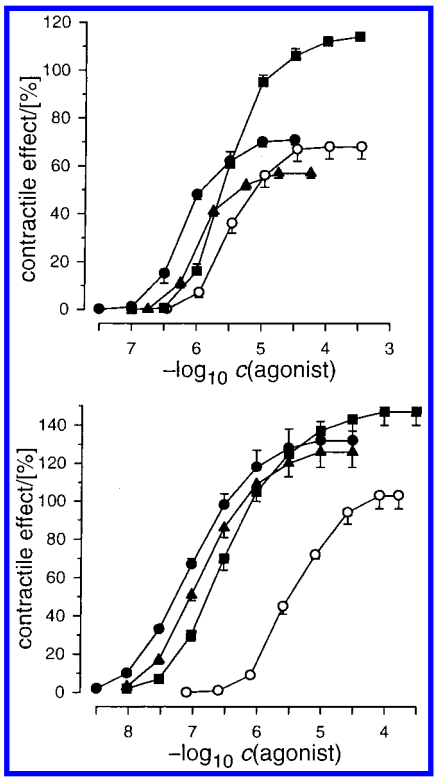

Figure 2. *Upper panel:* Contraction of guinea-pig aortic rings by histamine (■, $n = 17$, $E_{max} = 114 \pm 2\%$), **13** (●, $n = 12$, 71 ± 2%), and **14** (▲, $n = 12$, 57 ± 2%) in the absence of antagonist, and by **13** (○, $n = 5$, 68 ± 5%) in the presence of mepyramine (5 nM, 30 min, $pA_2 = 8.87 \pm 0.11$). Only second curves are shown. For pharmacological parameters of agonists, see Table 2. *Lower panel:* Contraction of guinea-pig aortic rings (precontracted with a threshold concentration of $PGF_{2\alpha}$) by histamine (■, $n = 13$, $E_{max} = 147 \pm 7\%$ relative to maximum response to 10 μM $PGF_{2\alpha}$), **13** (●, $n = 13$, 132 ± 10%), and **14** (▲, $n = 11$, 126 ± 8%) in the absence of antagonist, and by **13** (○, $n = 4$, 103 ± 7%) in the presence of mepyramine (100 nM, 60 min, $pA_2 = 8.75 \pm 0.07$). For pharmacological parameters of agonists, see Table 3.

in the guinea-pig ileum. Histaprodifen (**10**) and analogues **13**−**17** were partial agonists (relative $E_{max} \leq$ 62%). Their effect was sensitive to antagonism by mepyramine (Table 5, Figure 3 for **13**). However, the affinity of mepyramine was attenuated by 1 order of magnitude for all agonists studied ($pA_2 \approx 8$). This result is in line with reports on noticeably lower affinity of mepyramine in native rat tissues compared with guinea-pig or human preparations.[15] On the other hand, reduction of antagonist affinity vis-à-vis to rat H_1 receptors was not detected for homologues **11** and **12** ($pA_2 \approx 5.8$ compared to 6.0 on guinea-pig assays).

Interaction with Other Neurotransmitter Receptors. The histaprodifens **10** and **13**−**16** did not stimulate atrial H_2 receptors and ileal H_3 heteroreceptors of the guinea-pig. Their antagonist affinity at these sites was low (H_2: $pD'_2 < 5$) or not determinable (H_3: $pA_2 < 5.8$, or < 6.0 (**15**), or < 6.3 (**16**)) because micromolar affinity of **10** and **13**−**16** for cholinergic M_3 receptors in the ileum preparation prevented the use of higher antagonist concentrations (Table 6). The antagonist affinity of **10**, **13**, and **14** in several functional adrenoceptor and 5-HT-receptor assays was low ($pA_2 <$ 5.5) or not measurable (5-HT_3, 5-HT_4) due to the same reason described above for the H_3-receptor interaction. Agonist effects were not observed for **10**, **13**, and **14**.

Molecular Modeling

For a better understanding of structure−activity relationships, the interactions of histamine and the histaprodifens **10**, **13**, and **14** within the transmembrane (TM) domains of the human histamine H_1 receptor (hH1R) were studied using molecular dynamics (MD) simulations. To place the agonists into the putative receptor site, the experimentally detected interaction of the protonated nitrogen of the H_1-receptor agonists with Asp107 was used as a distance restraint. This residue is well conserved among biogenic amine receptors and is one of the most crucial amino acids for the binding of H_1-receptor agonists and antagonists.[41,42] A second group of constraints were set between the nitrogens of the imidazole ring and the upper part of TM V. These constraints reflect results of site directed mutagenesis studies showing a direct influence of Asn198 and Lys191 on the binding of histamine.[43−45] The last 100 ps of the

Table 4. Relaxation of Rat Aortic Rings (with Intact Endothelium, Submaximally Precontracted with 15.8 nM U46619) by Histamine and Histaprodifens **10**−**17**[a]

compd	N^b	pEC_{50} ± SEM	relative potency	(95% confidence limits)	E_{max} ± SEM (% carbachol)	E_{max} ± SEM[c] (% histamine)
10	9	6.07 ± 0.08	528	(330−847)	46 ± 4	50 ± 4
11	6		[pA_2 = 5.72 ± 0.14	(5.35−6.09)]	0	0[d]
12	6		[pA_2 = 5.97 ± 0.09	(5.75−6.20)]	0	0[d]
13	10	6.80 ± 0.07	2825	(1854−4305)	55 ± 5	61 ± 6
14	10	6.77 ± 0.04	2649	(1919−3656)	51 ± 3	55 ± 3
15	6	6.19 ± 0.07	684	(473−989)	44 ± 5	47 ± 6
16	12	6.45 ± 0.09	1250	(805−1941)	56 ± 3	62 ± 3
17	6	5.87 ± 0.05	331	(244−450)	21 ± 4	21 ± 4
histamine	18	5.35 ± 0.04	100		91 ± 2	100

[a] For structure, see Table 1. [b] Number of experiments. [c] Formerly termed 'intrinsic activity'.[48] Maximum of histamine controls (relative to maximum relaxation evoked by carbachol) arbitrarily set to 100%. [d] At 10 μM.

Table 5. Mepyramine Antagonism of Effects Evoked by **1** and Histaprodifens **10** and **13**−**17**[a] in Guinea-Pig (gp) and Rat Tissues

	gp ileum (contraction)			gp aorta (contraction)			gp aorta ($PGF_{2\alpha}$) (contraction)			rat aorta (relaxation)		
agonist	N^b	pA_2 ± SEM[c]	c^d	N^b	pA_2 ± SEM[c]	c^d	N^b	pA_2 ± SEM[c]	c^d	N^b	pA_2 ± SEM[c]	c^d
10	17	9.11 ± 0.04	*e*	4	8.80 ± 0.06	3	4	9.01 ± 0.11	10	6	8.04 ± 0.06	100
13	6	9.13 ± 0.06	3	6	8.87 ± 0.11	5	4	8.75 ± 0.07	100	8	8.02 ± 0.06	100
14	4	9.11 ± 0.12	3	6	8.86 ± 0.07	5	4	8.60 ± 0.05	100	6	7.98 ± 0.06	100
15	6	8.81 ± 0.08	5		ND			ND		3	*f*	100
16	5	8.85 ± 0.04	1	5	8.67 ± 0.07	10		ND		6	8.24 ± 0.03	50
17	2	9.02; 9.42	1		ND			ND		3	*f*	100
histamine	29	9.07 ± 0.03	*g*	34	9.11 ± 0.02	*h*	8	9.00 ± 0.06	30	8	8.00 ± 0.07	100

[a] For structure of agonists, see Table 1. [b] Number of experiments. [c] Apparent pA_2 (see Experimental Section) unless otherwise indicated. [d] Concentration of mepyramine [nM]. [e] Full pA_2 value (1−30 nM, see Figure 1 (upper panel) and Experimental Section). [f] pA_2 not calculated. Relaxant effect was abolished by 100 nM mepyramine. [g] Full pA_2 value (0.3−100 nM), Schild plot slope 1 (0.97 ± 0.04, $P > 0.20$). [h] Full pA_2 value (1−1000 nM), Schild plot slope 1 (1.00 ± 0.02, $P > 0.50$). ND not done.

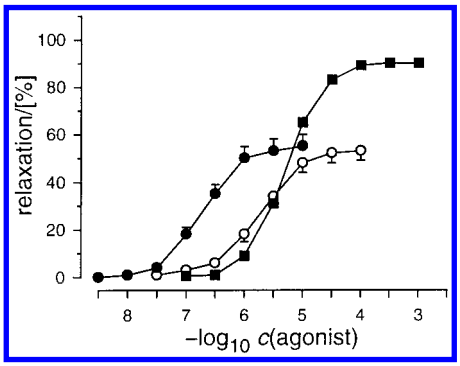

Figure 3. Relaxation of rat aortic rings with intact endothelium relative to maximum relaxation induced by carbachol (0.3−1 mM). Histamine (■, n = 12, E_{max} = 90 ± 2%) and methylhistaprodifen (**13**) (●, n = 10, 55 ± 5%) relaxed vascular preparations submaximally precontracted with 15.8 nM U46619 (a TP-receptor agonist). In the presence of mepyramine (100 nM, 75 min, pA_2 = 8.02 ± 0.06) the concentration−effect curve of **13** was shifted to the right (○, n = 8, 53 ± 4%). Only one curve was obtained from each preparation. For pharmacological parameters of agonists, see Table 4.

MD simulation were analyzed to characterize the interaction of the H_1-receptor agonists. The stability of the obtained ligand−receptor complexes was proved by a 1 ns MD simulation using tethering forces on the C_α-atoms of the protein backbone and removing all restraints between ligand and receptor for the last 750 ps.

Binding Model of Histamine. The histamine−hH1R complex having the lowest potential energy during the last 100 ps of MD is shown in Figure 4. The protonated nitrogen of the histamine alkyl chain strongly interacts with the carboxylic group of Asp107. The small deviations in distances (2.50 ± 0.07 Å for the last 100 ps) between the protonated nitrogen and the center of mass of the carboxylic group are a measure for the strength of this interaction. The alkyl chain is found to be in an extended conformation. In the MD simulation, histamine was able to form a stable hydrogen bond between the N^τ-H-atom[20] of the imidazole ring and the carbonyl oxygen of the Asn198 side chain in TM V (distance during last 100 ps: 2.08 ± 0.14 Å). This interaction is stabilized by an additional hydrogen bond between Asn198 and Tyr431. The N^π-atom[20] of the imidazole ring interacts with Lys191 forming a hydrogen bond. This locates the N^π-atom to the extracellular site of the receptor (see Figure 4a). Further, it was found that Thr194 does not play an important role in the binding of histamine. All these findings agree well with known experimental data on the binding of histamine to guinea-pig H_1-receptor mutants.[43,44] In our model, the complex is stabilized by Tyr108 and Phe435, making an aromatic stack with the imidazole ring. The 2-position of the imidazole ring is located close to TM V, and substitution of the imidazole ring in this position should yield a steric hindrance and cause a changed orientation of the imidazole ring. The protonated N^α-atom of histamine is closely located to TM III, forming hydrogen bonds with the carboxylic group of Asp107 and the backbone carbonyl oxygen of Leu104. This orientation makes all substitutions of the N^α-protons unfavorable because they influence either the interaction with the carboxylic group of Asp107 or are sterically hindered by Leu104. This corresponds to experimental data showing a decrease of agonist activity upon N^α-methylation of some histamine derivatives.[16]

The 1 ns MD simulation using the agonist−receptor complex shown in Figure 4 as starting structure shows a high stability of the histamine−hH1R interaction. The mean of the root-mean-square deviation (RMSD value,

Table 6. Functionally Determined Antagonist Affinity of Histaprodifens **10** and **13**−**16** for Histamine H_2, H_3, and Several Other Neurotransmitter Receptors[a]

		10		**13**		**14**		**15**		**16**	
receptor	(species[b])	pA_2[c] ± SEM	*c*(**10**) [μM]	pA_2[c] ± SEM	*c*(**13**) [μM]	pA_2[c] ± SEM	*c*(**14**) [μM]	pA_2[c] ± SEM	*c*(**15**) [μM]	pA_2[c] ± SEM	*c*(**16**) [μM]
H_2[d]	(gp)	4.46 ± 0.08	20	4.90 ± 0.02	20	4.58 ± 0.15	20	4.50 ± 0.11	20	4.70 ± 0.02	20
H_3[e,f]	(gp)	<5.8[g]	2	<5.8	1.6	<5.8	1	<6.0	1	<6.3[h]	0.5
M_3[i]	(gp)	5.55 ± 0.04	3−30	5.45 ± 0.03	3−30	5.94 ± 0.04	1−10	5.99 ± 0.06	1−10	6.03 ± 0.03	1−3
α_{1D}[e]	(r)	5.45 ± 0.10	10	5.24 ± 0.11	10	5.11 ± 0.04	20	ND		ND	
β_1[d]	(gp)	4.34 ± 0.06	30	4.84 ± 0.23	20; 30	4.58 ± 0.10	20	ND		ND	
5-HT_{1B}[e]	(gp)	4.85 ± 0.14	30	5.09 ± 0.08	30	<4.5	30	ND		ND	
5-HT_{2A}[e]	(r)	5.19 ± 0.05	20	5.39 ± 0.05	10	5.43 ± 0.09	10	ND		ND	
5-HT_3[e,f]	(gp)	<5.7	2	<5.8	1.6	<5.8	1.6	ND		ND	
5-HT_4[f,j]	(r)	<5.5	2	<5.8	1.6	<5.8	1.6	ND		ND	

[a] For structure of compounds, see Table 1. [b] *gp* = guinea-pig; *r* = rat. [c] Apparent pA_2 (see Experimental Section) except for H_2- and β_1-receptor assay (see footnote *d*). [d] pD'_2 value ± range/2,[50] $n = 2$. [e] $n = 4$−6. [f] Higher concentrations could not be tested with regard to the affinity of the compound for cholinergic M_3 receptors. [g] Dextral shift significant (0.22 log units, 95% confidence limit 0.08−0.35, $P < 0.02$); $pA_2 = 5.51$ (95% confidence limit 5.00−5.80). [h] Dextral shift significant (0.15 log units, 95% confidence limit 0.05−0.25, $P < 0.02$); $pA_2 = 5.92$ (95% confidence limit 5.40−6.20). [i] $n = 10$−13. [j] $n = 3$. ND not done.

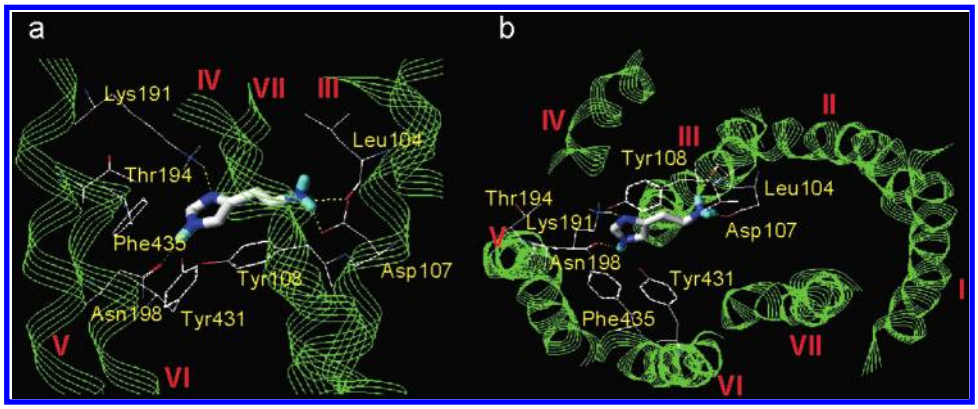

Figure 4. Binding model of histamine (**1**) in the TM region of the hH1R represented by a snapshot of the histamine−TM complex having the lowest potential energy (228 ps) during the last 100 ps of a 250 ps MD simulation. The complex is shown in different views: (a) view parallel to the TM domains, and (b) view from the extracellular side. It was found that Asp107, Leu104, Lys191, and Asn198 form stable hydrogen bonds to **1** (yellow dotted lines). The residues presented in this figure demonstrate that there is virtually no accessible surface around the agonist **1**. Red roman numerals describe the TM domains. The TM domain backbones are represented by green line ribbons.

measured every picosecond) of the histamine conformation compared with the structure presented in Figure 4 was found to be 1.189 Å during the last 500 ps of the MD simulation. This reflects the fact that all ligand−receptor interactions found were stable after removal of all restraints between histamine and the hH1R.

Binding Model of Histaprodifens. The histaprodifens **10**, **13**, and **14** presented in this work possess high agonist activity and enhanced receptor affinity compared with histamine. The common feature of these compounds is a space filling substituent in the 2-position of the imidazole ring. At present, no experimental information is available to characterize the binding pocket of histaprodifens. To derive a first hypothesis on the binding mode, the putative binding of N^{α}-unsubstituted (**10**), N^{α}-methyl- (**13**), and N^{α},N^{α}-dimethyl-substituted (**14**) histaprodifen in the TM domains of the hH1R was studied using MD. For the MD simulations the same restraints as described for histamine were used. The complex of **10** and the TM region of the hH1R is shown in Figure 5. The orientation of the imidazole ring differs substantially from that of histamine (see Figure 4). The carbonyl oxygen of the Asn198 side chain is able to form two hydrogen bonds with the N^{τ}-H-atom of the imidazole moiety and with the hydroxyl group of Tyr108. The N^{π}-atom forms a stable hydrogen bond with Tyr431 and cannot interact with Lys191. The different orientation of the imidazole ring is caused mainly by the space filling substitution in the 2-position. This result agrees with experimental data showing that the Lys200Ala mutant of the guinea-pig H_1 receptor, which is equivalent to Lys191 in the hH1R, attenuates the binding of histamine but has no impact on the binding of 2-(3-bromophenyl)histamine.[44] The imidazole ring of **10** is located near Phe435 (TM VI) and Tyr108 (TM III). The propyl group is responsible for the location of the phenyl rings deep in the hydrophobic pocket built by Phe199 (TM V), Pro202 (TM V), Phe432 (TM VI), Trp428 (TM VI), Trp158 (TM IV), Ile115 (TM III), and Tyr108 (TM III). Both phenyl rings fill out the space of the receptor pocket, and obviously no space is available to substitute them with residues much larger than hydrogen. This impression is supported by the experimental fact that efforts to increase the potency of **10** by substitution of the benzene rings have failed.[46]

The distance between the geometric centers of the imidazole nucleus and both benzene rings of **10** is found to be quite stable during the last 500 ps of a 1 ns dynamics (6.52 ± 0.20 Å for the distance to the geometric center of the first benzene ring and 7.28 ± 0.12 Å for the distance to the second benzene ring). The conformational analysis of **9**, a lower homologue of **10**, using the systematic search option (all C−C bonds in the 2-alkyl chain were defined as rotatable, step width

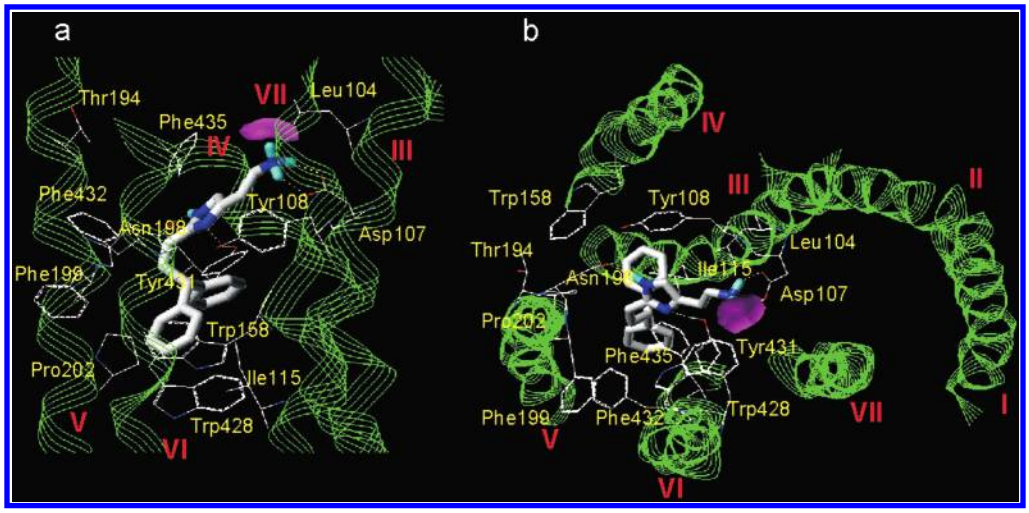

Figure 5. Binding model of histaprodifen (**10**) (226 ps, lowest potential energy conformation during the last 100 ps of a 250 ps MD simulation). The view parallel to the TM domains (a) shows that both phenyl rings of **10** are located deeply in the putative binding pocket built by TM domains III, IV, V, and VI (see b: view from the extracellular side). The monocation of **10** forms hydrogen bonds to Asp107, Asn198, and Tyr431 (yellow dotted lines). The surface near the protonated N^{α}-atom represents the only accessible surface area (magenta) of bound **10**. The TM domain backbones numbered in red (roman numerals) are represented by green line ribbons.

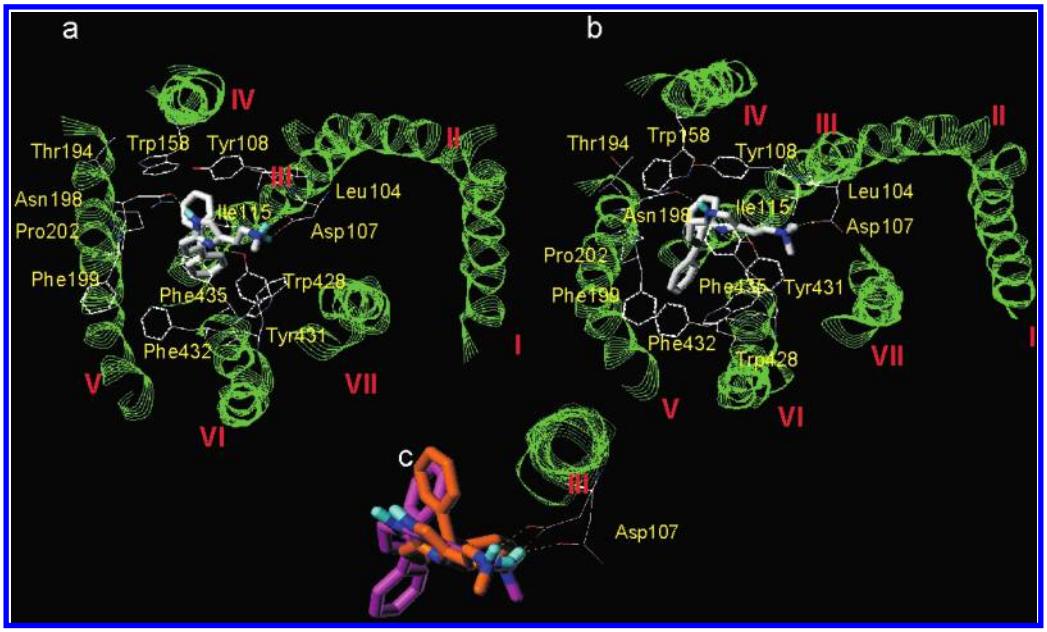

Figure 6. Binding models of methylhistaprodifen (**13**) (part a, 232 ps, lowest potential energy conformation during the last 100 ps of a 250 ps MD simulation, view from extracellular side) and dimethylhistaprodifen (**14**) (part b, 230 ps, lowest potential energy conformation during the last 100 ps of a 250 ps MD simulation, view from extracellular side). Both agonists form hydrogen bonds to Asp107, Asn198, and Tyr431 (yellow dotted lines). The orientation of all other residues except Asp107 is similar in parts a and b of Figure 6. The N^{α}-methyl group is located at the place represented by the accessible surface area of bound histaprodifen (see Figure 5). The different interaction of **13** (all carbon atoms colored orange) and **14** (all carbon atoms colored magenta) is presented more detailed in part c. The additional methyl substitution present in **14** yields a different location of both the Asp107 side chain and the N^{α}-atom.

15°) of SYBYL (Tripos Inc., St. Louis, 1999) shows that for a shortened alkyl chain the distance between the centers of the imidazole ring and the phenyl substituents is too small (5.18 ± 0.68 Å and 5.83 ± 0.59 Å) to localize both phenyl groups in the hydrophobic pocket. Conformational analysis for a longer alkyl chain between the imidazole ring and the benzene rings (viz. compound **11**) indicates that both phenyl substituents can only adopt the optimum position when the alkyl chain is folded (7.46 ± 0.95 Å and 7.28 ± 0.98 Å). In this model, such a folding leads to a sterical hindrance of the imidazole ring interaction with Asn198 and/or Tyr431. As a result, the model is in agreement with in vitro data presented for the lower (**8**, **9**) and higher (**11**, **12**) homologues of **10**.

The different orientation of imidazole rings having a space filling substitution in the 2-position causes a slightly changed location of the protonated N^{α}-atom within the receptor pocket. In contrast to the situation for histamine, the protonated positively charged N^{α}-atom of **10** is more exposed to the central pocket built by TM III, TM VI, and TM VII, and it does not form a hydrogen bond to the backbone of TM III. The accessible surface area of the NH_3^+-group of **10** (probe radius 1.4 Å) shown in Figure 5 indicates that one N^{α}-hydrogen can be replaced. This agrees with the binding model

calculated for methylhistaprodifen (**13**, Figure 6a). A comparison of the models shows that both **10** and **13** bind similarly, forming the same interactions with the hH1R. The additional N^{α}-methyl group does not change the interactions with Asp107 and increases the hydrophobic contacts with the receptor. The binding model of dimethylhistaprodifen (**14**) is presented in Figure 6b. Presumably the dimethyl substitution is responsible for a translocation of the N^{α}-atom closer to TM VII. In this model, **14** forms one hydrogen bond to the carboxylic group of Asp107. The space filling substitution is accompanied by a new orientation of the Asp107 side chain between TM III and TM VII which is more similar to that proposed for the binding of H_1-receptor antagonists.[43] This might explain the lower intrinsic activity of **14** compared with **10** and **13** in some of the in vitro assays.

Again the 1 ns MD simulations using the agonist−receptor complexes shown in Figures 5 and 6 as starting structures show a high stability of the agonist−hH1R interactions. The mean RMSD values for the calculated conformations of **10**, **13**, and **14** compared with the structures presented in Figures 5 and 6 were 1.693, 1.024, and 1.645 Å, respectively, during the last 500 ps of the MD simulation. Thus, all ligand−receptor interactions found were regarded as stable after removal of all restraints between agonist and hH1R.

Conclusion

Histaprodifen (**10**, 2-[2-(3,3-diphenylpropyl)-1*H*-imidazol-4-yl]ethanamine) and N^{α}-methylated derivatives **13** and **14** have been identified as attractive members of a new family of lead structures which may offer starting points for the systematic development of highly potent and selective histamine H_1-receptor agonists. Methylhistaprodifen (**13**) is the most potent H_1-receptor agonist known so far in the literature with relative functional potencies of 3.4-fold (guinea-pig ileum), 4.6- and 4.1-fold (two guinea-pig aorta assays), and 28-fold (rat aorta), and an affinity increased by 2 orders of magnitude compared with histamine. A plausible and stable binding model demonstrating the affinity-contributing interaction of the 3,3-diphenylpropyl moiety of histaprodifens as well as the effect of N^{α}-methylation on functional activity has been developed by means of molecular dynamics simulations using electron-density maps of frog rhodopsin, a G-protein coupled receptor, as a template.[27] Histaprodifens may be valuable tools for the investigation of H_1-receptor-mediated physiological and pathophysiological functions. Recently, two in vivo studies with pithed and anaesthetized rats have provided evidence that **10** and, in particular, **13** and **14** are highly potent H_1-receptor agonists.[47]

Experimental Section

Chemistry. General Procedures. Melting points were determined on an Electrothermal IA 9000 digital apparatus and are uncorrected. IR spectra were recorded on a Perkin-Elmer 1420 spectrometer. ^{1}H NMR spectra were recorded on a Bruker Avance-TM-DPX 400 (400 MHz) spectrometer. Chemical shifts are given in ppm downfield from TMS as internal reference. ^{1}H NMR data are reported in the order: multiplicity (s, singlet; d, doublet; t, triplet; q, quartet; m, multiplet; br, broad; *, exchangeable by D_2O), approximate coupling constant *J*, number of protons, and location of protons (Im, imidazole; Ph, phenyl; Mal, maleic acid; Pyr, pyrrolidine). Mass spectra were recorded using a Finnigan MAT CH7A (70 eV, EI spectra) or a Finnigan MAT CH5DF ($^+$FAB spectra). Elemental analyses (C, H, N, Vario EL) were within ±0.4% of the theoretical values. Yields were not optimized. Chromatographic separation was achieved by column chromatography using silica gel 60 (Merck No. 9285, 230-400 mesh). Preparative rotatory layer chromatography was performed using a Chromatotron 7924T (Harrison Research, CA) and glass rotors with 4 mm layers of silica gel 60 PF_{254} containing gypsum (Merck).

3,3-Diphenylpropionitrile (4a). Following a slightly modified published procedure,[29] commercially available 3,3-diphenylpropionic acid was treated with excess $SOCl_2$, followed by conversion of the product in liquid ammonia in an autoclave at ambient temperature. Dehydration with P_4O_{10} led to the desired material which had analytical and spectroscopical properties virtually identical with those reported.[29]

***ω,ω*-Diphenylalkanenitriles 4b−d. General Procedure.** To a suspension of potassium (4.3 g, 110 mmol) and catalytical amounts of $Fe(NO_3)_3$ in liquid NH_3 (100 mL, −70 °C) was added a solution of diphenylmethane (16.8 g, 100 mmol) in dry Et_2O (50 mL) dropwise over 15 min. The deep red suspension was stirred for 30 min, and a solution of *ω*-bromo- or *ω*-chloroalkanenitrile (100 mmol) in dry Et_2O (40 mL) was added. After the disappearance of the deep red color, NH_3 was allowed to evaporate. The organic layer was separated and the residue extracted twice with Et_2O (40 mL). The combined extracts were washed with 0.1 N HCl (2× 50 mL), water (100 mL), and brine (50 mL) and dried over Na_2SO_4. The solvent was removed under reduced pressure and the resulting oil purified by column chromatography using CH_2Cl_2/petrolether (40/60) as eluent.

4,4-Diphenylbutyronitrile (4b): yield 38%; mp 36 °C (petrolether); ^{1}H NMR ($CDCl_3$) δ 7.38−7.25 (m, 10H, 10 Ph-H), 4.12 (t, J = 8.0 Hz, 1H, CH), 2.47−2.41 (m, 2H, CHCH_2), 2.30 (t, J = 7.1 Hz, 2H, CH_2CN); $^+$FAB-MS (Xe, DMSO/*m*-NO_2-benzyl-OH) *m*/*z* 222 ([M + H]$^+$, 39), 183 (6), 167 (100), 144 (72); IR (KBr) 2245 cm^{-1} (CN). Anal. ($C_{16}H_{15}N$) C, H, N.

5,5-Diphenylvaleronitrile (4c): yield 59%; colorless oil; ^{1}H NMR ($CDCl_3$) δ 7.30−7.17 (m, 10H, 10 Ph-H), 3.90 (t, J = 7.8 Hz, 1H, CHCH$_2$), 2.33 (t, J = 7.0 Hz, 2H, CH_2CN), 2.24−2.17 (m, 2H, CHCH_2), 1.66−1.59 (m, 2H, CHCH_2CH_2); EI-MS *m*/*z* 235 (M$^{+\bullet}$, 12), 182 (24), 168 (11), 167 (100), 165 (15); IR (KBr) 2245 cm^{-1} (CN). Anal. ($C_{17}H_{17}N$) C, calcd 86.8, found 86.2; H, calcd 7.28, found 7.97; N, calcd 5.95, found 5.87.

6,6-Diphenylcapronitrile (4d): yield 59%; colorless oil; ^{1}H NMR ($CDCl_3$) δ 7.38−7.24 (m, 10H, 10 Ph-H), 3.97 (t, J = 7.8 Hz, 1H, CHCH$_2$), 2.24 (t, J = 7.2 Hz, 2H, CH_2CN), 2.17−2.08 (m, 2H, CHCH_2), 1.69 (tt, $J_1 = J_2$ = 7.4 Hz, 2H, CH_2CH$_2$CN), 1.50−1.42 (m, 2H, CHCH$_2$CH_2); EI-MS *m*/*z* 249 (M$^{+\bullet}$, 12), 182 (3), 168 (11), 167 (100), 152 (9), 128 (2), 105 (7); IR (KBr) 2245 cm^{-1} (CN). Anal. ($C_{18}H_{19}N$) C, H, N.

5,5-Diphenylvaleronitrile (4c). Alternative Synthesis. 3,3-Diphenylpropionic acid (12.6 g, 56 mmol) was converted to the corresponding propanol derivative by treatment with $LiAlH_4$ (2.3 g, 60 mmol) in dry Et_2O according to standard methods, followed by purification via column chromatography (CH_2Cl_2/MeOH (1/1)): yield 98%; colorless oil. Anal. ($C_{15}H_{16}O$) C, H. 3,3-Diphenyl-1-propanol (11.5 g, 54 mmol) and $SOCl_2$ (10 mL) were heated for 4 h in CH_2Cl_2 (20 mL) in the presence of a catalytic amount of 4-DMAP. The crude 1-chloro-3,3-diphenylpropane was isolated according to standard methodology and purified by column chromatography (petrolether): yield 90%; colorless oil. Anal. ($C_{15}H_{15}Cl$) C, H. To a suspension of NaH (2.0 g suspension in mineral oil, 50 mmol) and catalytic amounts of NaI in dry DMF (60 mL) was added a solution of diethyl malonate (10 g, 63 mmol) in dry DMF (30 mL). When the formation of H_2 had ceased, a solution of 1-chloro-3,3-diphenylpropane (10.9 g, 47 mmol) was added slowly. After having been stirred for 2 h at 60 °C the mixture was heated to 90 °C for additional 36 h. After cooling and pouring into water (300 mL), the mixture was extracted with Et_2O (3 × 70 mL). After separation of the organic layers and evaporation, the organic residue was dissolved in a solution of KOH (10 g),

water (30 mL), and EtOH (20 mL) and refluxed for 12 h. After the mixture cooled to ambient temperature, impurities were separated by extraction with Et_2O (50 mL). The aqueous layer was diluted with 3 N NaOH (100 mL) and extracted with Et_2O (2× 50 mL). After rejecting the organic layer, the aqueous phase was acidified with 6 N H_2SO_4. After extraction with Et_2O (3 × 70 mL) and removal of the solvent under reduced pressure, 2-(3,3-diphenylpropyl)malonic acid was obtained which was used for the next step without further purification: yield 47%; pale yellow semisolid. $C_{18}H_{18}O_4$. Heating of the malonic acid derivative (6.5 g, 22 mmol) at 180 °C in vacuo for 10 min followed by cooling led to a residue which was dissolved in a mixture of 3 N NaOH (100 mL) and MeOH (50 mL). The basic solution was extracted twice with petrolether/Et_2O (1/1) and acidified by addition of 6 N H_2SO_4, and the product was extracted with Et_2O (3 × 70 mL). After removal of the organic solvent under reduced pressure, 5,5-diphenylvaleric acid was isolated without further purification: yield 74%; pale brown oil. $C_{17}H_{18}O_2$. 5,5-Diphenylvaleric acid (4.0 g, 16 mmol), dissolved in dry CH_2Cl_2 (20 mL), was added to a solution of chlorosulfonylisocyanate[30] (3.1 g, 22 mmol) in dry CH_2Cl_2 (30 mL) and refluxed for 4 h. After addition of 0.5 N NaOH (100 mL), the organic layer was separated, the aqueous phase was extracted with CH_2Cl_2 (2 × 50 mL), and the combined organic layers were dried (Na_2SO_4) and evaporated to dryness. Column chromatography of the residue (petrolether/CH_2Cl_2 (60/40)) led to **4c**: yield 52%; colorless oil. Spectral data were virtually identical with those reported above. All intermediates described in this paragraph gave satisfactory ^{1}H NMR and mass spectra.

Methyl Imidate Hydrochlorides 5a−d. General Method. A solution of **4a−d** (37.5 mmol) in dry MeOH (30 mL) was chilled to −30 °C. After the solution was stirred for 5 min, $SOCl_2$ (3.0 mL, 42 mmol) was added to the solution. After 5 days in a freezer the solvent was removed in vacuo. The bulk was pure enough for the subsequent imidazole synthesis and was used without further purification. For the preparation of **5b**, the semisolid bulk was repeatedly evaporated after addition of dry Et_2O until a dry amorphous solid was obtained. Compound **5a** was immediately converted without analytical characterization.

Methyl 4,4-Diphenylbutyrimidate Hydrochloride (5b): yield 94%; mp 104 °C; ^{1}H NMR (CD_3OD) δ 7.32−7.14 (m, 10H, 10 Ph-H), 4.02−3.97 (m, 4H, OC*H*$_3$, C*H*CH$_2$), 2.64 (t, J = 7.6 Hz, 2H, C*H*$_2$C(=NH$_2^+$)OCH$_3$), 2.52−2.47 (m, 2H, CHC*H*$_2$); $^+$FAB-MS (Xe, DMSO/*m*-NO_2-benzyl-OH) *m*/*z* 254 ([M + H]$^+$, 100), 239 (3), 167 (10). $C_{17}H_{19}NO\cdot HCl$.

Methyl 5,5-Diphenylvalerimidate Hydrochloride (5c): yield 96%; ^{1}H NMR (CD_3OD) δ 7.29−7.13 (m, 10H, 10 Ph-H), 3.94 (t, J = 7.8 Hz, 1H, C*H*CH2), 3.32 (s, 3H, OCH$_3$), 2.24 (t, J = 7.4 Hz, 2H, C*H*$_2$C(=NH$_2^+$)OCH$_3$), 2.12−2.07 (m, 2H, CHC*H*$_2$), 1.62−1.54 (m, 2H, CHCH$_2$C*H*$_2$); $^+$FAB-MS (Xe, DMSO/*m*-NO_2-benzyl-OH) *m*/*z* 268 ([M + H]$^+$, 100), 167 (11), 165 (10), 117 (20), 100 (100). $C_{18}H_{21}NO\cdot HCl$.

Methyl 6,6-Diphenylcaproimidate Hydrochloride (5d): yield 87%; $^+$FAB-MS (Xe, glycerol) *m*/*z* 283 ([M + 2H]$^{2+}$, 20), 205 (12), 168 (13), 167 (68), 91 (100). $C_{19}H_{23}NO\cdot HCl$.

2-[2-(3,3-Diphenylpropyl)-1*H*-imidazol-4-yl]ethanol (6). 2-Oxobutan-1,4-diol[31] (15.6 g, 150 mmol) and **5b** (10.2 g, 35 mmol) were dissolved in liquid NH_3 (100 mL) in an autoclave (1000 mL, Kotter, Germany) and converted as described for compound **10**. After evaporation of NH_3 the residue was poured into CH_2Cl_2 (300 mL) and washed with water (3 × 100 mL). The solvent was distilled off, and the product was purified by column chromatography using CH_2Cl_2/MeOH/triethylamine (95/4/1) as eluent. The resulting yellow oil (**6**) was pure enough for further reactions. An analytical sample was crystallized as hydrogen oxalate from EtOH/Et_2O: yield 5.0 g (46%); mp 149 °C; ^{1}H NMR ($CDCl_3$) δ 7.26−7.11 (m, 10H, 10 Ph-H), 6.57 (s, 1H, Im-5-H), 6.21 (s*, 1H, OH), 3.87 (t, J = 7.7 Hz, 1H, C*H*CH$_2$), 3.78 (t, J = 5.9 Hz, 2H, C*H*$_2$OH), 2.73 (t, J = 5.9 Hz, 2H, Im-C$_{(4)}$-CH$_2$), 2.59−2.55 (m, 2H, Im-C$_{(2)}$-CH$_2$), 2.45−2.39 (m, 2H, CHC*H*$_2$); EI-MS *m*/*z* 306 (M$^{+\bullet}$, free base, 2), 202 (30), 165 (11), 126 (100). Anal. ($C_{20}H_{22}N_2O\cdot C_2H_2O_4$) C, H, N.

2-(3,3-Diphenylpropyl)-4-(2-chloroethyl)-1*H*-imidazole (7). To a solution of **6** (4.5 g, 14.7 mmol) in CH_2Cl_2 (30 mL) was slowly added $SOCl_2$ (10 mL, 137 mmol) under ice cooling. The mixture was stirred for 1 h at ambient temperature and then refluxed for 2 h. The solvent was removed under reduced pressure and the resulting oil taken up in Et_2O, washed with 0.1 N NaOH, water, and brine. After evaporation and purification by column chromatography, **7** was obtained as a light brown oil: yield 3.2 g (60%). An analytical sample was crystallized as hydrogen oxalate from EtOH/Et_2O: mp 159 °C; ^{1}H NMR ($CDCl_3$) δ 8.77 (br*, 1H, NH), 7.28−7.15 (m, 10H, 10 Ph-H), 6.69 (s, 1H, Im-5-H), 3.89 (t, J = 7.8 Hz, 1H, C*H*CH$_2$), 3.74 (t, J = 6.9 Hz, 2H, CH$_2$Cl), 2.99 (t, J = 7.0 Hz, 2H, Im-C$_{(4)}$-CH$_2$), 2.64−2.60 (m, 2H, Im-C$_{(2)}$-CH$_2$), 2.50−2.44 (m, 2H, CHC*H*$_2$); $^+$FAB-MS (Xe, DMSO/*m*-NO_2-benzyl-OH) *m*/*z* 325 ([M + H]$^+$, 100), 289 (12), 220 (7). Anal. ($C_{20}H_{21}N_2Cl\cdot C_2H_2O_4$) C, H, N.

Synthesis of 2-[2-(*ω*,*ω*-Diphenylalkyl)-1*H*-imidazol-4-yl]ethanamines 9−12. General Method. 2-Oxo-4-phthalimido-1-butyl acetate[32] (4.0 g, 15 mmol) and **5a−d** (14 mmol) were dissolved in liquid NH_3 (150 mL) in an autoclave (1000 mL, Kotter, Germany). After being stirred for 12 h at room temperature the mixture was heated to 60 °C (24−26 bar) for 6 h. Then NH_3 was allowed to evaporate, and the residue was dissolved in MeOH (100 mL). Hydrazine hydrate (1.0 g, 20 mmol) was added, and the solution was refluxed for 3 h. The solvent was removed, and the free base extracted with CH_2Cl_2/MeOH (3 × 50 mL). After rotatory chromatography (CH_2Cl_2/MeOH (10/1), NH_3-saturated) the base was obtained. Crystallization with maleic acid from EtOH/Et_2O afforded the dihydrogen maleate salts of **9−12**.

2-[2-(2,2-Diphenylethyl)-1*H*-imidazol-4-yl]ethanamine Dihydrogen Maleate (9): yield 22%; mp 159 °C; ^{1}H NMR (DMSO-d_6) δ 7.30−7.16 (m, 11H, 10 Ph-H, Im-5-H), 6.08 (s, 4H, 4 Mal-H), 4.59 (t, J = 8.3 Hz, 1H, C*H*CH$_2$), 3.62 (t, J = 8.3 Hz, 2H, Im-C$_{(2)}$-CH$_2$), 3.01 (t, J = 7.3 Hz, 2H, CH$_2$C*H*$_2$N), 2.80 (t, J = 7.8 Hz, 2H, Im-C$_{(4)}$-CH$_2$); $^+$FAB-MS (Xe, DMSO/*m*-NO_2-benzyl-OH) *m*/*z* 292 ([M + H]$^+$, 100), 275 (9), 263 (6), 167 (61). Anal. ($C_{19}H_{21}N_3\cdot 2C_4H_4O_4$) C, H, N.

2-[2-(3,3-Diphenylpropyl)-1*H*-imidazol-4-yl]ethanamine Dihydrogen Maleate (10, Histaprodifen): yield 5%; mp 148−150 °C; ^{1}H NMR (CD_3OD) δ 7.30−7.19 (m, 10H, 10 Ph-H), 7.16 (s, 1H, Im-5-H), 6.27 (s, 4H, 4 Mal-H), 4.01 (t, J = 7.8 Hz, 1H, C*H*CH$_2$), 3.24 (t, J = 7.5 Hz, 2H, CH$_2$C*H*$_2$N), 2.99 (t, J = 7.5 Hz, 2H, Im-C$_{(4)}$-CH$_2$), 2.89 (t, J = 7.8 Hz, 2H, Im-C$_{(2)}$-CH$_2$), 2.60−2.54 (m, 2H, CHC*H*$_2$); $^+$FAB-MS (Xe, DMSO/glycerol) *m*/*z* 306 ([M + H]$^+$, 100), 289 (8), 277 (8). Anal. ($C_{20}H_{23}N_3\cdot 2C_4H_4O_4$) C, H, N.

2-[2-(4,4-Diphenylbutyl)-1*H*-imidazol-4-yl]ethanamine Dihydrogen Maleate (11): yield 3%; mp 135 °C; ^{1}H NMR (CD_3OD) δ 7.30−7.15 (m, 10H, 10 Ph-H), 7.21 (s, 1H, Im-5-H), 6.27 (s, 4H, 4 Mal-H), 3.96 (t, J = 7.8 Hz, 1H, C*H*CH$_2$), 3.25 (t, J = 7.5 Hz, 2H, CH$_2$C*H*$_2$N), 3.02 (t, J = 7.5 Hz, 2H, Im-C$_{(4)}$-CH$_2$), 2.94 (t, J = 7.8 Hz, 2H, Im-C$_{(2)}$-CH$_2$), 2.18−2.13 (m, 2H, CHC*H*$_2$), 1.76−1.73 (m, 2H, CHCH$_2$C*H*$_2$); $^+$FAB-MS (Xe, DMSO/*m*-NO_2-benzyl-OH) *m*/*z* 321 ([M + 2H]$^{2+}$, 25), 320 ([M + H]$^+$, 100), 303 (9), 291 (9). Anal. ($C_{21}H_{25}N_3\cdot 2C_4H_4O_4$) C, H, N.

2-[2-(5,5-Diphenylpentyl)-1*H*-imidazol-4-yl]ethanamine Dihydrogen Maleate (12): yield 5%; mp 120−121 °C; ^{1}H NMR (CD_3OD) δ 7.27−7.11 (m, 11H, 10 Ph-H, Im-5-H), 6.25 (s, 4H, 4 Mal-H), 3.90 (t, J = 7.8 Hz, 1H, C*H*CH$_2$), 3.25 (t, J = 7.5 Hz, 2H, CH$_2$C*H*$_2$N), 3.02 (t, J = 7.5 Hz, 2H, Im-C$_{(4)}$-CH$_2$), 2.86 (t, J = 7.7 Hz, 2H, Im-C$_{(2)}$-CH$_2$), 2.09 (dt, J_1 = J_2 = 7.7 Hz, 2H, CHC*H*$_2$), 1.82 (tt, J_1 = J_2 = 7.6 Hz, 2H, CHCH$_2$CH$_2$C*H*$_2$), 1.34−1.28 (m, 2H, CHCH$_2$C*H*$_2$); $^+$FAB-MS (Xe, DMSO/*m*-NO_2-benzyl-OH) *m*/*z* 335 ([M + 2H]$^{2+}$, 28), 334 ([M + H]$^+$, 100), 317 (9), 305 (7), 167 (9). Anal. ($C_{22}H_{27}N_3\cdot 2C_4H_4O_4\cdot 0.5H_2O$) C, H, N.

***N*$^{\alpha}$-Substituted Histaprodifens 13−17. General Procedure.** To a mixture of **7** (0.49−0.65 g, 1.5−2 mmol), K_2CO_3 (0.4 g, 3 mmol), the respective amine (10−20 mmol of free base, dissolved in EtOH), and catalytical amounts of KI in EtOH (30 mL) was added H_2O until a clear solution was obtained.

The mixture was then heated to reflux for 2−4 h. The solvents were evaporated in vacuo and the free bases extracted with CH_2Cl_2. After rotatory chromatography (CH_2Cl_2/MeOH (10/1), NH_3-saturated) the purified free bases were obtained. Crystallization with oxalic acid from EtOH afforded dihydrogen oxalates **13**−**17**.

***N*-Methyl-2-[2-(3,3-diphenylpropyl)-1*H*-imidazol-4-yl]-ethanamine Dihydrogen Oxalate (13):** yield 57%; mp 207 °C (dec); ^{1}H NMR (CD_3OD) δ 7.31−7.18 (m, 11H, 10 Ph-H, Im-5-H), 4.01 (t, J = 7.8 Hz, 1H, C*H*CH$_2$), 3.39 (m, 2H, C*H*$_2$-NCH$_3$), 3.05 (t, J = 7.5 Hz, 2H, Im-C$_{(4)}$-CH$_2$), 2.90 (t, J = 7.5 Hz, 2H, Im-C$_{(2)}$-CH$_2$), 2.77 (s, 3H, NCH$_3$), 2.57 (m, 2H, CHC*H*$_2$); $^+$FAB-MS (Xe, DMSO/glycerol) m/z 320 ([M + H]$^+$, 100), 289 (27), 277 (50). Anal. ($C_{21}H_{25}N_3$·2$C_2H_2O_4$) C, H, N.

***N*,*N*-Dimethyl-2-[2-(3,3-diphenylpropyl)-1*H*-imidazol-4-yl]ethanamine Dihydrogen Oxalate (14):** yield 47%; mp 158 °C; ^{1}H NMR (CD_3OD) δ 7.30−7.17 (m, 11H, 10 Ph-H, Im-5-H), 4.01 (t, J = 7.8 Hz, 1H, C*H*CH$_2$), 3.39 (t, J = 7.7 Hz, 2H, CH$_2$N), 3.11 (t, J = 7.6 Hz, 2H, Im-C$_{(2)}$-CH$_2$), 2.93−2.75 (m, 8H, Im-C$_{(4)}$-CH$_2$, N(CH$_3$)$_2$), 2.58 (m, 2H, CHC*H*$_2$); $^+$FAB-MS (Xe, DMSO/glycerol) m/z 334 ([M + H]$^+$, 100), 289 (23). Anal. ($C_{22}H_{27}N_3$·2$C_2H_2O_4$) C, H, N.

***N*-Ethyl-2-[2-(3,3-diphenylpropyl)-1*H*-imidazol-4-yl]-ethanamine Dihydrogen Oxalate (15):** yield 51%; mp 207−209 °C (dec); ^{1}H NMR (DMSO-d_6) δ 7.33−7.17 (m, 10H, 10 Ph-H), 7.04 (s, 1H, Im-5-H), 3.99 (t, J = 7.7 Hz, 1H, C*H*CH$_2$), 3.14 (t, J = 7.4 Hz, 2H, C*H*$_2$NC$_2$H$_5$), 2.97 (q, J = 7.2 Hz, 2H, NC*H*$_2$CH$_3$), 2.85 (t, J = 7.3 Hz, 2H, Im-C$_{(4)}$-CH$_2$), 2.64 (t, J = 7.3 Hz, 2H, Im-C$_{(2)}$-CH$_2$), 2.50−2.42 (m, 2H, CHC*H*$_2$), 1.18 (t, J = 7.2 Hz, 3H, NCH$_2$C*H*$_3$); $^+$FAB-MS (Xe, DMSO/glycerol) m/z 334 ([M + H]$^+$, 100), 289 (16), 277 (52). Anal. ($C_{22}H_{27}N_3$·2$C_2H_2O_4$) C, H, N.

***N*-Cyclopropyl-2-[2-(3,3-diphenylpropyl)-1*H*-imidazol-4-yl]ethanamine Dihydrogen Oxalate (16):** yield 51%; mp 200−201 °C (dec); ^{1}H NMR (DMSO-d_6) δ 7.33−7.27 (m, 8H, 8 Ph-H), 7.19−7.16 (m, 2H, 2 Ph-H), 7.12 (s, 1H, Im-5-H), 3.99 (t, J = 7.7 Hz, 1H, C*H*CH$_2$), 3.24 (t, J = 7.6 Hz, 2H, C*H*$_2$NCH), 2.90 (t, J = 7.5 Hz, 2H, Im-C$_{(4)}$-CH$_2$), 2.70−2.67 (m, 3H, CH$_2$-NC*H*, Im-C$_{(2)}$-CH$_2$), 2.49−2.43 (m, 2H, CHC*H*$_2$), 8.81−0.69 (m, 4H, NCHC$_2$*H*$_4$); $^+$FAB-MS (Xe, DMSO/*m*-NO$_2$-benzyl-OH) m/z 347 ([M + 2H]$^{2+}$, 27), 346 ([M + H]$^+$, 100), 277 (11). Anal. ($C_{23}H_{27}N_3$·2$C_2H_2O_4$) C, H, N.

2-(3,3-Diphenylpropyl)-4-(2-pyrrolidinoethyl)-1*H*-imidazole Dihydrogen Oxalate (17): yield 52%; mp 195−197 °C (dec); ^{1}H NMR (DMSO-d_6) δ 7.33−7.27 (m, 8H, 8 Ph-H), 7.20−7.16 (m, 2H, 2 Ph-H), 7.09 (s, 1H, Im-5-H), 5.23 (br*, 2H, 2 COOH), 3.99 (t, J = 7.7 Hz, 1H, C*H* CH$_2$), 3.35 (t, J = 7.7 Hz, 2H, CH$_2$Pyr), 3.26 (m, 4H, 4 Pyr-H), 2.94 (t, J = 7.7 Hz, 2H, Im-C$_{(4)}$-CH$_2$), 2.67 (m, J = 7.8 Hz, 2H, Im-C$_{(2)}$-CH$_2$), 2.51−2.43 (m, 2H, CHC*H*$_2$), 1.92 (m, 4H, 4 Pyr-H); $^+$FAB-MS (Xe, DMSO/*m*-NO$_2$-benzyl-OH) m/z 361([M + 2H]$^{2+}$, 21), 360 ([M + H]$^+$, 73), 318 (3) 289 (10), 276 (5), 84 (100); Anal. ($C_{24}H_{29}N_3$·2$C_2H_2O_4$) C, H, N.

Pharmacology. Data Handling and Pharmacological Parameters. Data are presented as mean ± standard error (SEM or SE) or with 95% confidence limits. Graphical data (Figures 1−3) are given as mean ± SEM (SEM does not appear when smaller than symbol). Significant differences of means or the difference of a mean from a constant value ($P < 0.05$) were discerned by Student's t test. Agonists were characterized by relative potency compared with histamine, calculated as antilog of (pEC$_{50}$(agonist) − pEC$_{50}$(histamine)). The first concentration−effect curve (CEC) for histamine served as an internal reference when two CECs were performed on each preparation. The daily mean of untreated histamine control organs served as reference when only one CEC per organ was established. E_{max} [%] of the new agonists (formerly termed *intrinsic activity*[48]) was calculated relative to histamine. The negative logarithm of the dissociation constant of the partial-agonist/receptor complex, pK_P, was calculated from individual sets of equieffective concentrations of histamine in the absence and presence of a maximal or supramaximal concentration of partial agonist.[35] When pK_P values were determined at different partial agonist concentrations, the overall pK_P was calculated by a Kaumann-Marano plot[36] after constraining the slope of the regression line to unity. The affinity of the H_1-receptor antagonist mepyramine was calculated as pA_2 from experiments with histamine or the new agonists in the absence or presence of suitable concentrations of mepyramine. Apparent pA_2 values were obtained from experiments with a single mepyramine concentration according to the equation pA_2 = −log c(mepyramine) + log (r − 1), where r is the ratio of agonist concentrations in the presence and absence of mepyramine that elicit 50% of the respective maximum effect.[49] When a set of at least three different mepyramine concentrations was studied, full pA_2 values were calculated from Arunlakshana-Schild plots after constraining the Schild plot slope to unity.[34] Contractile effects evoked by very weak agonists (**8**, **9**) were qualitatively blocked by 100 nM mepyramine. Apparent pA_2 values of compounds devoid of agonist properties vis-à-vis to H_1 receptors (**11**, **12**) were determined as described above for mepyramine. Antagonist potencies of the new compounds at selected neurotransmitter receptor subtypes were calculated as apparent pA_2 values (see above) or as pD'_2 values,[50] when only depression of CECs instead of rightward displacement was observed.

Histamine H_1-Receptor Assay on the Isolated Guinea-Pig Ileum. Guinea-pigs of either sex were stunned by a blow on the head and exsanguinated. The ileum was removed, and whole segments (2.0−2.5 cm) were mounted isotonically (preload 0.5 g) at 37 °C in Tyrode's solution,[51] aerated with 95% O_2/5% CO_2, in the continuous presence of 0.1 μM atropine, a concentration not affecting H_1 receptors.[21] During an equilibration period of ca. 80 min, the organs were stimulated three times with histamine (1 and 10 μM) followed by washout. Each preparation was used to establish a cumulative concentration−effect curve for histamine (0.01−30 μM) followed either by a second curve for a new agonist in the absence or presence of mepyramine (1−100 nM, incubation time 10−15 min), or by a second histamine curve in the presence of antagonist (incubation time 10 min). The pEC$_{50}$ difference was not corrected since two successive curves for histamine were superimposable (n = 10). For the determination of pK_P, the partial agonist was not washed out and incubated for 1−10 min (see Table 1). A final cumulative curve for histamine was then constructed.

Histamine H_1-Receptor Assay on the Isolated Endothelium-Denuded Guinea-Pig Aorta. Thoracic aortae of sacrificed guinea-pigs were quickly removed and cleared of connective tissue. Rings of 2−4 mm length were cut and rolled with a pair of tweezers to damage the endothelium. Organs were mounted isometrically (initial tension 10 mN) by means of two L-shaped stainless steel hooks in a modified Krebs-Henseleit solution (37 °C, gassed with 95% O_2/5% CO_2, 1.80 mM Ca^{2+}, 1.20 mM Mg^{2+}). During an equilibration period of ca. 130 min, organs were stimulated three times with histamine (10 μM) followed by washout. Cumulative concentration−effect curves for histamine (0.1−300 μM) followed by a second curve for histamine or a new agonist in the absence or presence of mepyramine (1−1000 nM, incubation time 30 min) or antagonist (incubation time 30 min) were established in the presence of cimetidine, corticosterone, cocaine (30 μM each), prazosin, yohimbine (0.3 μM each), and propranolol (0.1 μM). The pEC$_{50}$ difference was corrected using the sensitivity change monitored by untreated histamine control preparations.

Histamine H_1-Receptor Assay on the Isolated Endothelium-Denuded Guinea-Pig Aorta, Precontracted with a Threshold Concentration of $PGF_{2\alpha}$. Preparations were set up as described in the preceding paragraph. After a stabilization period of 100 min, the organs were challenged twice (duration 20 and 45 min) with $PGF_{2\alpha}$ (10 μM), followed by washout each. Before the final cumulative concentration−effect curve with histamine (0.01−300 μM) or a new agonist in the absence or presence of mepyramine (10−100 nM, total incubation time approximately 60 min) or antagonist was performed, the preparations were precontracted with a threshold concentration of $PGF_{2\alpha}$ (usually 0.4−1.5 μM) corresponding to 10−20% of the contraction evoked by 10 μM $PGF_{2\alpha}$ during

the second challenge. The contractile effect of histamine or the new agonists was expressed relative to the maximum obtained for 10 μM $PGF_{2\alpha}$ during the second challenge. The cocktail of six drugs mentioned in the preceding paragraph was present during the final curve and the second challenge with $PGF_{2\alpha}$.

Histamine H_1-Receptor Assay on the Isolated Rat Aorta with Intact Endothelium. Male Wistar rats were stunned (CO_2) and decapitated. The thoracic portion of the aorta was rapidly removed, rinsed, and cleared of connective tissue. Rings of 2−4 mm length were cut and set up isometrically (initial tension 10 mN) by means of two L-shaped stainless steel hooks in a modified Krebs-Henseleit solution (37 °C, gassed with 95% O_2/5% CO_2, 1.25 mM Ca^{2+}, 1.20 mM Mg^{2+}). After an equilibration period of ca. 100 min, vascular rings were contracted with a submaximal concentration of U46619, a TP(thromboxane-A_2)-receptor agonist (15.8 nM) in the presence of prazosin (100 nM). When the effect had plateaued (usually after 45 min), a cumulative concentration−relaxation curve was established for histamine (0.1−1000 μM) or a new agonist in the absence or presence of mepyramine (100 nM, total incubation time approximately 75 min). Potential H_1-receptor antagonists were studied like mepyramine versus histamine. When the agonist had elicited its maximum effect, a final relaxation was induced by addition of the M_3-receptor agonist carbachol (300−1000 μM).

Histamine H_2-Receptor Assay on the Isolated Spontaneously Beating Guinea-Pig Right Atrium. The right atrium was set up isometrically (initial tension 5 mN) as described.[51] Cumulative concentration−frequency curves for histamine in the absence and presence of the studied compounds were obtained in the continuous presence of 0.3 μM propranolol and 1 μM mepyramine.

Histamine H_3-Receptor Assay on the Isolated Electrically Stimulated Guinea-Pig Ileal Longitudinal Muscle with Adhering Plexus Myentericus. Segments of ileal longitudinal muscle were set up isometrically (initial tension 7.5 mN) as described.[52] Cumulative concentration−effect curves for (*R*)-α-methylhistamine in the absence and presence of the studied compounds (incubated for 20 min at concentrations not interfering with muscarinic M_3 receptors) were obtained in the continuous presence of 1 μM mepyramine.

Antagonist Activity of Title Compounds at Non-Histamine Receptors. Experiments were performed according to published protocols for the following functional receptor assays: Muscarinic M_3 receptors of guinea-pig whole ileal segments[51] (in the presence of 1 μM mepyramine), adrenergic α_{1D} receptors of rat thoracic aorta,[51] and β_1 receptors of spontaneously beating guinea-pig right atrium[51] (in the presence of 1 μM mepyramine), serotonergic 5-HT_{1B} receptors of guinea-pig arteria iliaca[51] (in the presence of 1 μM mepyramine), 5-HT_{2A} receptors of rat tail artery,[51] 5-HT_3 receptors of quiescent guinea-pig ileal longitudinal muscle with adhering plexus myentericus[53] (in the presence of 1 μM mepyramine), and 5-HT_4 receptors of rat oesophagal tunica muscularis mucosae,[53] respectively. For the new compounds, agonist effects were not observed in all non-H_1-receptor assays.

Molecular Modeling. Modeling of the Histamine H_1 Receptor. The human histamine H_1 receptor (hH1R) belongs to the rhodopsin family of G-protein coupled receptors. This allows to use the α-carbon template of the transmembrane (TM) helices[54] based on a three-dimensional electron-density map of frog rhodopsin with an effective resolution of 7.5 Å in the membrane plane.[27] Highly conserved amino acids in each of the TM domains permit unambiguous alignment of the primary sequence of rhodopsin with the histamine H_1 receptors. The starting structure of hH1R TM domains was built using the biopolymer tool of the program package SYBYL 6.4 (Tripos Inc.). *N*-Acetyl and *N*-methyl groups were added to the N- and C-termini of the TM helices. The model of the hH1R TM region was minimized using the sander module of AMBER 4.1[55] (cutoff for nonbonded interactions 12 Å, conjugate gradient minimization, RMS-gradient cutoff 0.01).

RESP Charge Calculations. The original Amber 4.1 was parametrized and equilibrated with ab initio derived charges (6-31G* basis set) calculated using the restrained electrostatic potential fitting method RESP.[56] This method avoids the designation of excessively large point charges to buried atoms. The application of RESP yields a force field consistent calculation of electrostatic potentials and intermolecular interaction energies. The atomic charges of ligands used in this modeling study were calculated using the RESP formalism. The ab initio UHF type energy calculations (NGAUSS = 6, GBASIS = N31, POLAR = POPLE) were performed with the program GAMESS_US.[57] Molecular electrostatic potentials were calculated from GAMESS_US output with MOLDEN 3.2[58] and used as input for RESP to obtain force field consistent point charges for the histaminergic agonists. This procedure leads to identical results comparable with original AMBER 4.1 charge calculations (ter Laak and Kühne, unpublished results). The histamine derivatives are able to exist in three differently protonated states (uncharged, with one protonated imidazole nitrogen; monocation, with additional protonated side chain amino group; dication, in which all nitrogens are protonated). Both the uncharged and the monocation form are able to undergo tautomerism. In our modeling studies, we used the N^{τ}-monocation which is most likely the biologically active species.[59]

Molecular Dynamics (MD) Simulations. The minimized structure of the hH1R TM region represents only one local minimum strongly depending on the used α-carbon template.[54] In this template, the area enclosed by seven helices near the intracellular site is 25% smaller than near the extracellular site. Thus, the template represents mainly the inactive receptor state.[27] Therefore, an MD setup containing three phases was used: (i) Dynamic relaxation of the putative inactive state of hH1R TM domains with the agonist outside the TM region (100 ps), (ii) dynamic docking of H_1-receptor agonists into the putative active site of the receptor using distance restraints (50 ps), and (iii) dynamic relaxation of the agonist−receptor complex (100 ps). The arrangement of the seven-helix bundle was fixed by a set of distance restraints between the centers of three α-carbons in each helix (TM I: Val42, Thr41, Val40; TM II: Pro82, Met81, Val80; TM III: Ser114, Ala113, Thr112; TM IV: Pro161, Ile160, Val159; TM V: Pro202, Leu201, Tyr200; TM VI: Pro430, Ile429, Trp428; TM VII: Pro465, Asn464, Leu463). The definition of these distance restraints allows conformational changes during the whole MD simulation, like rotations of helices, kinks of helices near prolines, and different relative orientations of the TM domains. Therefore, this setup permits the simultaneous study of the relaxation of the inactive state of the seven-helix bundle, the conformational changes of the TM domains during agonist docking, and the relaxation of the agonist−receptor complex.[60] This reflects the known experimental fact that during the agonist-induced receptor activation rigid body motions of the seven TM domains occur.[61,62] The stability of the calculated agonist−receptor complexes was studied by 1 ns MD simulations using positional restraints of 10 kcal mol^{-1} $Å^{-2}$ on all receptor backbone C_α-atoms. After 250 ps all restraints between ligand and receptor were removed. To analyze the stability of the agonist−receptor complex, the mean RMSD value of the agonist conformation compared with the starting structure during the last 500 ps was calculated.

All MD simulations were carried out at 300 K in vacuo using the sander module of AMBER 4.1[55] (time step 2 fs using hydrogen atom bond 'SHAKE' option, dielectric constant ϵ = 1, cutoff for nonbonded interactions 12 Å, update of nonbonded pairs every 10 steps, and heat coupling of 0.2 ps). In vacuo MD simulations of TM domains yield a loss of helical content.[63] To stabilize the helical conformation of TM domains, all helical backbone hydrogen bonds were restrained using distance constraints with a force constant of 10 kcal mol^{-1} $Å^{-2}$.

Acknowledgment. This project was supported by Verband der Chemischen Industrie, Fonds der Chemie (Frankfurt/Main, Germany) (S.E., W.S.), and by the FNK of the Freie Universität Berlin (S.E., K.K.). The authors acknowledge the contribution of Inge Walther to some of the functional receptor selectivity experiments.

References

(1) Kramer, K.; Detert, H.; Leschke, C.; Elz, S.; Schunack, W. 2-(3,3-Diphenylpropyl)histamine: A Lead for Highly Potent H_1-Receptor Agonists. XXVIth Meeting of the European Histamine Research Society, Sevilla, Spain, May 14−17, 1997, Abstract No. 28.

(2) Kramer, K.; Detert, H.; Elz, S.; Pertz, H.; Schunack, W. A New Class of Selective and Highly Potent Histamine H_1-Receptor Agonists: N^{α}-Substituted Derivatives of Histaprodifen. XXVIIth Meeting of the European Histamine Research Society, Lódz, Poland, May 20−23, 1998, Abstract No. 38.

(3) Elz, S.; Kramer, K.; Pertz, H.; Schunack, W. Methylhistaprodifen and Congeners: Highly Potent and Selective Histamine H_1-Receptor Agonists. XIIIth International Congress of Pharmacology, Munich, Germany, July 26−31, 1998; *Naunyn-Schmiedeberg's Arch. Pharmacol.* **1998**, *358* (Suppl. 2), R762.

(4) Tuomisto, L.; Tacke, U. Is Histamine an Anticonvulsive Inhibitory Transmitter? *Neuropharmacology* **1986**, *25*, 955−958.

(5) Yokoyama, H.; Onodera, K.; Maeyama, K.; Yanai, K.; Iinuma, K.; Tuomisto, L.; Watanabe, T. Histamine Levels and Clonic Convulsions of Electrically-Induced Seizure in Mice: The Effects of α-Fluoromethylhistidine and Metoprine. *Naunyn-Schmiedeberg's Arch. Pharmacol.* **1992**, *346*, 40−45.

(6) Oishi, R.; Adachi, N.; Saeki, K. *N*-α-Methylhistamine Inhibits Intestinal Transit in Mice by Central Histamine H_1 Receptor Activation. *Eur. J. Pharmacol.* **1993**, *237*, 155−159.

(7) Toda, N. Mechanism of Histamine Actions in Human Coronary Arteries. *Circ. Res.* **1987**, *61*, 280−286.

(8) Matsanuyama, K.; Yasue, H.; Okumura, K.; Matsuyama, K.; Ogawa, H.; Morikami, Y.; Inotsume, N.; Nakano, M. Effects of H_1 Receptor Stimulation on Coronary Arterial Diameter and Coronary Hemodynamics in Humans. *Circulation* **1990**, *81*, 65−71.

(9) Okumura, K.; Yasue, H.; Matsuyama, K.; Morikami, Y.; Ogawa, H.; Obata, K. Effects of H_1 Receptor Stimulation on Coronary Artery Diameter in Patients with Varient Angina: Comparison with Effect of Acetylcholine. *J. Am. Coll. Cardiol.* **1991**, *17*, 338−345.

(10) Monti, J. M.; Jantos, H.; Leschke, C.; Elz, S.; Schunack, W. The Selective Histamine H_1-Receptor Agonist 2-(3-Trifluoromethylphenyl)histamine Increases Waking in the Rat. *Eur. Neuropsychopharmacol.* **1994**, *4*, 459−462.

(11) Durant, G. J.; Duncan, W. A. M.; Ganellin, C. R.; Parson M. E.; Blakemore, R. C.; Rasmussen, A. C. Impromidine (SK&F 92676) is a Very Potent and Specific Agonist for Histamine H_2 Receptors. *Nature (London)* **1978**, *276*, 403−405.

(12) Buschauer, A. Synthesis and In Vitro Pharmacology of Arpromidine and Related Phenyl(pyridylalkyl)guanidines, a Potential New Class of Positive Inotropic Drugs. *J. Med. Chem.* **1989**, *32*, 1963−1970.

(13) Arrang, J.-M.; Garbarg, M.; Lancelot, J.-C.; Lecomte, J.-M.; Pollard, H.; Robba, M.; Schunack, W.; Schwartz, J.-C. Highly Potent and Selective Ligands for Histamine H_3-Receptors. *Nature (London)* **1987**, *327*, 117−123.

(14) Garbarg, M.; Arrang, J.-M.; Rouleau, A.; Ligneau, X.; Trung Tuong, M. D.; Schwartz, J.-C.; Ganellin, C. R. S-[2-(4-Imidazolyl)-ethyl]isothiourea, a Highly Specific and Potent Histamine H_3 Receptor Agonist. *J. Pharmacol. Exp. Ther.* **1992**, *263*, 304−310.

(15) Hill, S. J.; Ganellin, C. R.; Timmerman, H.; Schwartz, J.-C.; Shankley, N. P.; Young, J. M.; Schunack, W.; Levi, R.; Haas, H. L. International Union of Pharmacology. XIII. Classification of Histamine Receptors. *Pharmacol. Rev.* **1997**, *49*, 253−278.

(16) Zingel, V.; Leschke, C.; Schunack, W. Developments in Histamine H_1-Receptor Agonists. *Prog. Drug Res.* **1995**, *44*, 49−85.

(17) Durant, G. J.; Ganellin, C. R.; Parsons, M. E. Chemical Differentiation of Histamine H_1- and H_2-Receptor Agonists. *J. Med. Chem.* **1975**, *18*, 905−909.

(18) Hepp, M.; Dziuron, P.; Schunack, W. Structure−Activity Relationships of Histamine Analogues. XIX. 2-Substituted Histamines with Selective H_1-Agonistic Activity. *Arch. Pharm. (Weinheim, Ger.)* **1979**, *312*, 637−639.

(19) Dziuron, P.; Schunack, W. Structure−Activity Relationships of Histamine Analogues. VIII. Synthesis and Activity of 2-Substituted Histamines. *Eur. J. Med. Chem. Chim. Ther.* **1975**, *10*, 129−133.

(20) For nomenclature see: Black, J. W.; Ganellin, C. R. Naming Substituted Histamines. *Experientia* **1974**, *30*, 111−113.

(21) Leschke, C.; Elz, S.; Garbarg, M.; Schunack, W. Synthesis and Histamine H_1 Receptor Agonist Activitiy of a Series of 2-Phenylhistamines, 2-Heteroarylhistamines, and Analogues. *J. Med. Chem.* **1995**, *38*, 1287−1294.

(22) Hepp, M.; Schunack, W. Structure−Activity Relationships of Histamine Analogues. XXI. Synthesis and Pharmacology of N^{α}-Substituted Histamines. *Arch. Pharm. (Weinheim, Ger.)* **1980**, *313*, 756−762.

(23) Kramer, K.; Elz, S.; Pertz, H. H.; Schunack, W. N^{α}-Alkylated Derivatives of 2-Phenylhistamine: Synthesis and *In-Vitro* Activity of Potent Histamine H_1-Receptor Agonists. *Bioorg. Med. Chem. Lett.* **1998**, *8*, 2583−2588.

(24) Detert, H.; Leschke, C.; Tögel, W.; Seifert, R.; Schunack, W. 2-Alkyl-Substituted Histamines and Hydroxyethylimidazoles with G-Protein-Stimulatory Activity. *Eur. J. Med. Chem.* **1996**, *31*, 397−405.

(25) Nürnberg, B.; Tögel, W.; Krause, G.; Storm, R.; Breitweg-Lehmann, E.; Schunack, W. Non-Peptide G-Protein Activators as Promising Tools in Cell Biology and Potential Drug Leads. *Eur. J. Med. Chem.* **1999**, *34*, 5−30.

(26) Handley, D. A.; Hong, Y.; Bakale, R.; Senanayake, C. Norastemizole. *Drugs Future* **1998**, *23*, 966−969.

(27) Unger, V. M.; Hargrave, P. A.; Baldwin, J. M.; Schertler, G. F. X. Arrangement of Rhodopsin Transmembrane α-Helices. *Nature (London)* **1997**, *389*, 203−206.

(28) Dziuron, P.; Schunack, W. A New Synthesis of Imidazole Derivatives. *Arch. Pharm. (Weinheim, Ger.)* **1973**, *306*, 347−350.

(29) Take, K.; Okumura, K.; Tsubaki, K.; Terai, T.; Shiokawa, Y. Agents for the Treatment of Overactive Detrusor. IV. Synthesis and Structure−Activity Relationships of Cyclic Analogues of Terodiline. *Chem. Pharm. Bull.* **1993**, *41*, 507−515.

(30) Vorbrüggen, H. Reactive Isocyanates. I. Direct Introduction of Nitrile Groups into Unsaturated Systems. Simple Conversion of Carboxylic Acids into Nitriles. *Tetrahedron Lett.* **1968**, *13*, 1631−1634.

(31) Reppe, W. IV. Ethynylation. *Justus Liebigs Ann. Chem.* **1955**, *596*, 38−79.

(32) Zingel, V.; Elz, S.; Schunack, W. Histamine Analogues. XXXIII. 2-Phenylhistamines with High Histamine H_1-Agonistic Activity. *Eur. J. Med. Chem.* **1990**, *25*, 673−680.

(33) Kenakin, T. P.; Cook, D. A. *N,N*-Diethyl-2-(1-pyridyl)ethylamine, a Partial Agonist for Histamine Receptors in Guinea Pig Ileum. *Can. J. Physiol. Pharmacol.* **1980**, *58*, 1307−1310.

(34) Arunlakshana, O.; Schild, H. O. Some Quantitative Uses of Drug Antagonists. *Br. J. Pharmacol. Chemother.* **1959**, *14*, 48−58.

(35) Marano, M.; Kaumann, A. J. On the Statistics of Drug-Receptor Constants for Partial Agonists. *J. Pharmacol. Exp. Ther.* **1976**, *198*, 518−525.

(36) Kaumann, A. J.; Marano, M. On Equilibrium Dissociation Constants for Complexes of Drug-Receptor Subtypes. Selective and Non-Selective Interactions of Partial Agonists with Two Plausible β-Adrenoceptor Subtypes Mediating Positive Chronotropic Effects of (−)-Isoprenaline in Kitten Atria. *Naunyn-Schmiedeberg's Arch. Pharmacol.* **1982**, *318*, 192−201.

(37) Dodel, R.; Borchard, U. The Affinity of Antihistamines to Peripheral Histamine H_1-Receptors. *Agents Actions* **1992**, *37*, C410−C413.

(38) Van der Voorde, J.; Leusen, I. Vascular Endothelium and the Relaxation Effect of Histamine on Aorta of the Rat. *Arch. Int. Pharmacodyn. Ther.* **1982**, *256*, 329−330.

(39) Van der Voorde, J.; Leusen, I. Role of the Endothelium in the Vasodilator Response of Rat Thoracic Aorta to Histamine. *Eur. J. Pharmacol.* **1983**, *87*, 113−120.

(40) Carrier, G. O.; White, R. E.; Kirby, M. L. Histamine-Induced Relaxation of Rat Aorta. Importance of H_1 Receptor and Vascular Endothelium. *Blood Vessels* **1984**, *21*, 180−183.

(41) Ohta, K.; Hayashi, H.; Mizuguchi, H.; Kagamiyama, H.; Fujimoto, K.; Fukui, H. Site-Directed Mutagenesis of the Histamine H_1 Receptor: Roles of Aspartic Acid107, Asparagine198 and Threonine194. *Biochem. Biophys. Res. Commun.* **1994**, *203*, 1096−1101.

(42) Nonaka, H.; Otaki, S.; Oshima, E.; Kono, M.; Kase, H.; Ohta, K.; Fukui, H.; Ichimura, M. Unique Binding Pocket for KW-4679 in the Histamine H_1 Receptor. *Eur. J. Pharmacol.* **1998**, *345*, 111−117.

(43) Ter Laak, A. M.; Timmerman, H.; Leurs, R.; Nederkoorn, P. H. J.; Smit, M. J.; Donné-Op den Kelder, G. M. Modeling and Mutation Studies on the Histamine H_1 Receptor Agonist Binding Site Reveal Different Binding Modes for H_1-Agonists: Asp116 (TM3) Has a Constitutive Role in Receptor Stimulation. *J. Comput. Aided Mol. Des.* **1995**, *9*, 319−330.

(44) Leurs, R.; Smit, M. J.; Tensen, C. P.; ter Laak, A. M.; Timmerman, H. Lys200 Located in the Fifth Transmembrane Domain of the Histamine H_1 Receptor Interacts with Histamine but not with All H_1 Agonists. *Biochem. Biophys. Res. Commun.* **1994**, *201*, 295−301.

(45) Moguilevsky, N.; Varsolana, F.; Guillaume, J.-P.; Noyer, M.; Gillard, M.; Daliers, J.; Henichart, J.-P.; Bollen, A. Pharmacological and Functional Characterisation of the Wild-Type and Site-Directed Mutants of the Human H_1 Histamine Receptor Stably Expressed in CHO Cells. *J. Recept. Signal Transduction Res.* **1995**, *15*, 91−102.

(46) Elz, S.; Kramer, K.; Leschke, C.; Schunack, W. Ring-Substituted Histaprodifen Analogues as Partial Agonists for Histamine H_1 Receptors: Synthesis and Structure−Activity Relationships. *Eur. J. Med. Chem.* **2000**, *35*, 1−12.

(47) Malinowska, B.; Piszcz, J.; Schlicker, E.; Kramer, K.; Elz, S.; Schunack, W. Histaprodifen, Methylhistaprodifen, and Dimethylhistaprodifen are Potent H_1-Receptor Agonists in the Pithed and in the Anaesthetized Rat. *Naunyn-Schmiedeberg's Arch. Pharmacol.* **1999**, *359*, 11−16.
(48) Jenkinson, D. H.; Barnard, E. A.; Hoyer, D.; Humphrey, P. P. A.; Leff, P.; Shankley, N. P. International Union of Pharmacology Committee on Receptor Nomenclature and Drug Classification. IX. Recommendations on Terms and Symbols in Quantitative Pharmacology. *Pharmacol. Rev.* **1995**, *47*, 255−266.
(49) Furchgott, R. F. The Classification of Adrenoceptors (Adrenergic Receptors). In *Catecholamines, Handbook of Experimental Pharmacology*, vol. 33; Blaschko, H., Muscholl, E., Eds.; Springer: Berlin, 1972; pp 283−335.
(50) Van Rossum, J. M. Cumulative Dose−Response Curves. II. Technique for the Making of Dose−Response Curves in Isolated Organs and the Evaluation of Drug Parameters. *Arch. Int. Pharmacodyn. Ther.* **1963**, *143*, 299−330.
(51) Pertz, H.; Elz, S. In−Vitro Pharmacology of Sarpogrelate and the Enantiomers of its Major Metabolite: 5-HT_{2A} Receptor Specificity, Stereoselectivity and Modulation of Ritanserin-Induced Depression of 5-HT Contractions in Rat Tail Artery. *J. Pharm. Pharmacol.* **1995**, *47*, 310−316.
(52) Sasse, A.; Kiec-Kononowicz, K.; Stark, H.; Motyl, M.; Reidemeister, S.; Ganellin, C. R.; Ligneau, X.; Schwartz, J.-C.; Schunack, W. Development of Chiral *N*-Alkylcarbamates as New Leads for Potent and Selective H_3-Receptor Antagonists: Synthesis, Capillary Electrophoresis, and In Vitro and Oral In Vivo Activity. *J. Med. Chem.* **1999**, *42*, 593−600.
(53) Elz, S.; Keller, A. Preparation and In Vitro Pharmacology of 5-HT_4 Receptor Ligands. Partial Agonism and Antagonism of Metoclopramide Analogous Benzoic Esters. *Arch. Pharm. Pharm. Med. Chem.* **1995**, *328*, 585−594.
(54) Baldwin, J. M.; Schertler, G. F. X.; Unger, V. M. An Alpha-Carbon Template for the Transmembrane Helices in the Rhodopsin Family of G-Protein Coupled Receptors. *J. Mol. Biol.* **1997**, *272*, 144−154.
(55) Pearlman, D. A.; Case, D. A.; Caldwell, J. W.; Ross, W. S.; Cheatham, T. E., III; Ferguson, D. M.; Seibel, G. L.; Singh, U. C.; Weiner, P. K.; Kollman, P. A. AMBER 4.1, University of California, San Francisco, USA, 1995.
(56) Bayly, C. I.; Cieplak, P.; Cornell, W. D.; Kollman, P. A. A Well Behaved Electrostatic Potential Based Method Using Charge Restraints for Deriving Atomic Charges: The RESP Model. *J. Phys. Chem.* **1993**, *102*, 3787−3793.
(57) Schmidt, M. W.; Baldridge, K. K.; Boatz, J. A.; Elbert, S. T.; Gordon, M. S.; Jensen, J. H.; Koseki, S.; Matsunage, N.; Nguyen, K. A.; Su, S. J.; Windus, T. L.; Dupuis, M.; Montgomery, J. A. General Atomic and Molecular Electronic Structure System. *J. Comput. Chem.* **1993**, *14*, 1347−1363.
(58) Schaftenaar, G. MOLDEN: A Portable Electron Density Progam (QCPE619). *Quantum Chemical Program Exchange Bulletin* **1992**, *12*, 3.
(59) Zhang, M. Q.; Leurs, R.; Timmerman, H. Histamine H_1-Receptor Antagonists. In *Burger's Medicinal Chemistry and Drug Discovery, Therapeutic Agents*, 5th ed., Vol. 2; Wolff, M. E., Ed.; Wiley & Sons: New York, 1997; pp 495−559.
(60) Anders, J.; Blüggel, M.; Meyer, H. E.; Kühne, R.; ter Laak, A. M.; Kojro, E.; Fahrenholtz, F. Direct Identification of the Agonist Binding Site in the Human Brain Cholecystokinin$_B$ Receptor. *Biochemistry* **1999**, *38*, 6043−6055.
(61) Farrens, D. L.; Altenbach, C.; Yang, K.; Hubbell, W. J.; Khorana, H. G. Requirement of Rigid-Body Motion of Transmembrane Helices for Light Activation of Rhodopsin. *Science* **1996**, *274*, 768−770.
(62) Gether, U.; Kobilka, B. Fluorescent Labeling of Purified Beta 2 Adrenergic Receptor. Evidence for Ligand-Specific Conformational Changes. *J. Biol. Chem.* **1995**, *270*, 28267−28275.
(63) Ter Laak, A. M.; Kühne, R. Bacteriorhodopsin in a Periodic Boundary Water-Vacuum-Water Box as an Example Towards Stable Molecular Dynamics Simulations of G-Protein Coupled Receptors. *Recept. Channels* **1999**, *6*, 295−308.

JM991056A